# GIM violation and new dynamics of the third generation

Gerhard Buchalla,[1,*] Gustavo Burdman,[1,†] C. T. Hill,[1,‡] and Dimitris Kominis[2,§]
[1]*Fermi National Accelerator Laboratory, P. O. Box 500, Batavia, Illinois 60510*
[2]*Institut für Theoretische Physik, Technische Universität München, James-Franck-Strasse, 85748 Garching, Germany*
(Received 26 October 1995)

In strong dynamical schemes for electroweak symmetry breaking the third generation must be treated in a special manner, owing to the heavy top quark. This potentially leads to new flavor physics involving the members of the third generation in concert with the adjoining generations, with potential novel effects in $b$-flavored and charm physics. We give a general discussion and formulation of this kind of physics, abstracted largely from top-color models which we elaborate in detail. We identify sensitive channels for such new physics accessible to current and future experiments.

PACS number(s): 12.60.Cn, 12.15.Ff, 12.15.Ji, 12.60.Nz

## I. INTRODUCTION

The problem of understanding the origin of electroweak symmetry breaking is far from solved. The fermion Dirac masses arise in conjunction with the electroweak symmetry breaking since the left-handed members have weak isospin $I=1/2$ while the right-handed members have $I=0$. While the lightest quarks and leptons can be regarded as perturbative spectators to the electroweak dynamics, the very massive top quark suggests that it, and thus the third generation, are potentially enjoying a more intimate role in the electroweak dynamics and/or horizontal symmetry breaking. A potential implication of this is the possibility that there exist new fermion interactions that do not treat the generations in an egalitarian manner *at the electroweak scale*. If there are dynamical distinctions between the generations at the electroweak scale, then there is the possibility of new observable phenomena which violate the Glashow-Iliopoulos-Maiani (GIM) structure of the standard model interactions. An example is any description in which electroweak symmetry breaking is dynamical, in analogy with chiral symmetry breaking in QCD, such as technicolor (TC) and extended technicolor (ETC) [1]. These approaches require special treatment of the large top-quark mass generation. Various mechanisms for a large top-quark mass have been proposed, including the walking TC [2], subcritical amplification [3], two-scale technicolor [4], and top-color [5–7].

In the present paper we will focus on top-color, because it is fairly well defined within the context of the existing fermionic generations, and has direct implications of the general kind we wish to consider. However, we view it as generic in the possible new GIM-violating effects that it generates. Thus, we use top-color in the present paper as a generating mechanism for possible signals of new physics that might arise in detailed observations of, mostly, $b$ and $c$ quark weak processes. Top-color assumes that most of the top-quark mass arises from a $tt$ condensate. Previously, top-quark condensation models tried to identify all of the electroweak symmetry breaking (ESB) with the formation of a dynamical top quark mass [8], but this requires a very large scale for the new dynamics $\Lambda\sim 10^{15}$ GeV and significant fine-tuning. In top-color we assume naturalness, i.e., the scale of the new physics is $\sim 1$ TeV, and thus we estimate the decay constant of the associated top pions by using the Pagels-Stokar formula in the Nambu–Jona-Lasinio approximation [8]. This gives

$$f_\pi^2=\frac{N_c}{16\pi^2}m_c^2\left(\ln\frac{\Lambda^2}{m_c^2}+k\right), \tag{1}$$

where $m_c$ is the dynamical mass, $k$ a constant of order 1, and $\Lambda$ the cutoff scale at which the dynamical mass is rapidly going to zero. This results in $f_\pi\sim 50$ GeV, a decay constant too small to account for all of the electroweak symmetry breaking, which requires $f_\pi=174$ GeV. Hence we must postulate that top-color is occurring in tandem with some other mechanism that gives most of the electroweak scale. This means that the top-pions are not the longitudinal $W$ and $Z$, but are separate, physically observable objects. The top-pions must thus be massive, so in addition to the top-color model the top quark must derive some of its mass (about $\sim 3\%$) from the electroweak breaking, allowing $m_{\tilde{\pi}}\sim 200$ GeV.

''Top-color assisted technicolor'' was sketched out in [6]. The specific model presented in [6] was based upon the gauge group $\mathrm{SU}(3)_1\times\mathrm{SU}(3)_2\times\mathrm{U}(1)_{Y1}\times\mathrm{U}(1)_{Y2}\times\mathrm{SU}(2)_L$, where the strong double $\mathrm{U}(1)_{Yi}$ structure is required to tilt the chiral condensate in the $tt$ direction, and not form a $bb$ condensate. We shall refer to schemes based upon this gauge structure, containing an additional U(1), as top-color I models. Potentially serious problems with the $T$ parameter can arise [9] in this scheme owing to the strong coupled U(1), but they are avoided by judicious choice of representations in technicolor, and reasonably complete models have been constructed [10].

In the present paper we give a discussion of the dynamical features of top-color I models, building upon the recent work of one of us [11]. One of our main goals is to provide an effective Lagrangian for the full bound-state dynamics. This provides a natural starting point for the discussion of other

*Electronic address: buchalla@fnth20.fnal.gov
†Electronic address: burdman@fnth22.fnal.gov
‡Electronic address: hill@fnal.gov
§Electronic address: kominis@physik.tu-muenchen.de

 

potentially observable effects. One intriguing result is that the $\theta$ term in the top-color model can be the origin of observed $CP$ violation, yielding the Cabibbo-Kobayashi-Maskawa (CKM) phase in the standard model and a Jarlskog determinant of the right magnitude.

The potentially observable effects we are interested in arise because in the current basis of quarks and leptons the third generation experiences new strong forces. When we diagonalize the mass matrix to arrive at the mass basis there will be induced flavor-changing interactions. Some of these have been previously discussed [6,11]. Effects such as $BB$ mixing are potentially dangerous. The first- and second-generational mixing effects are suppressed because the third generation is somewhat isolated, and these effects involve high powers of small mixing angles. Top-color, to an extent, explains the suppression of the $3\rightarrow 2,1$ mixing angles, though without further assumptions about the origin of generational structure it cannot distinguish between 1 and 2.

We will sketch how the top-color scheme can impose textures upon the mass matrix which has important consequences for observable processes. Textures are inevitable when there are gauge quantum numbers that distinguish generations. A chiral-triangular texture seems to emerge as a natural possibility, and this can suppress dangerous processes such as $BB$ mixing.

The top-color I models will be discussed in the context of the implications for GIM violation and new flavor physics. Here the additional U(1) gives rise to semileptonic processes of interest. The model in this truncated sector is somewhat akin to Holdom's generational $Z'$ model, with similar implications [12]. We will also present a class of models, top-color II (essentially based upon [5]), built upon the gauge group $\mathrm{SU}(3)_Q\times\mathrm{SU}(3)_1\times\mathrm{SU}(3)_2\times\mathrm{U}(1)_Y\times\mathrm{SU}(2)_L$, where there is only the conventional $\mathrm{U}(1)_Y$, and no strong additional U(1). These models have several desirable features and have a rather intriguing anomaly cancellation solution in which the $(c,s)_{L,R}$ doublets are treated differently under the strong $\mathrm{SU}(3)_1\times\mathrm{SU}(3)_2$ structure. This leads to potentially interesting implications for charm physics in sensitive experiments.

Section IV of the paper deals with the phenomenological signatures of the new dynamics. It can be read independently of the theoretical discussions. We identify interesting sensitivities in some nonleptonic process such as $BB$ and $DD$ mixing, and radiative processes such as $b\rightarrow s\gamma$. However, we find that, in general, the strong dynamics at the TeV scale is difficult to observe in nonleptonic modes. On the other hand, the semileptonic modes we identify are interesting and sensitive to the $Z'$ of the top-color I schemes (as well as in other $Z'$ schemes). In general, top-color dynamics remains viable at the current level of sensitivity and poses interesting experimental challenges in high-statistics heavy-flavor experiments.

## II. TOP-COLOR DYNAMICS

### A. Models with a strong U(1) to tilt the condensate (top-color I)

We consider the possibility that the top-quark mass is large because it is a combination of a *dynamical condensate component*, $(1-\epsilon)m_t$, generated by a new strong dynamics, together with a small *fundamental component*, $\epsilon m_t$, i.e., $\epsilon\ll 1$, generated by an extended technicolor (ETC) or Higgs sector. The new strong dynamics is assumed to be chiral, critically strong but spontaneously broken, perhaps by TC itself, at the scale $\sim 1$ TeV, and it is coupled preferentially to the third generation. The new strong dynamics therefore occurs primarily in interactions that involve $\overline{tttt}$, $\overline{tt}\,\overline{bb}$, and $\overline{bbbb}$, while the ETC interactions of the form $\overline{ttQQ}$, where $Q$ is a techniquark, are relatively feeble.

Our basic assumptions leave little freedom of choice in the new dynamics. We assume a new class of technicolor models incorporating ''top-color'' (TopC). In TopC I the dynamics at the $\sim 1$ TeV scale involves the structure (or a generalization thereof)

$$\mathrm{SU}(3)_1\times\mathrm{SU}(3)_2\times\mathrm{U}(1)_{Y1}\times\ \mathrm{U}(1)_{Y2}\times\mathrm{SU}(2)_L \rightarrow \mathrm{SU}(3)_{\mathrm{QCD}}\times\mathrm{U}(1)_{\mathrm{EM}}, \tag{2}$$

where $\mathrm{SU}(3)_1\times\mathrm{U}(1)_{Y1}$ $[\mathrm{SU}(3)_2\times\mathrm{U}(1)_{Y2}]$ generally couples preferentially to the third (first and second) generations. The $\mathrm{U}(1)_{Yi}$ are just strongly rescaled versions of electroweak $\mathrm{U}(1)_Y$. We remark that employing a new $\mathrm{SU}(2)_{L,R}$ strong interaction in the third generation is also thinkable, but may be problematic due to potentially large instanton effects that violate $B+L$. We will not explore this latter possibility further.

The fermions are then assigned $(\mathrm{SU}(3)_1,\ \mathrm{SU}(3)_2,\ Y_1,\ Y_2)$ quantum numbers in the following way:

$$\begin{gathered}(t,b)_L\sim(3,1,1/3,0),\quad (t,b)_R\sim[3,1,(4/3,-2/3),0],\\ (\nu_\tau,\tau)_L\sim(1,1,-1,0),\quad \tau_R\sim(1,1,-2,0),\\ (u,d)_L,(c,s)_L\sim(1,3,0,1/3),\\ (u,d)_R,(c,s)_R\sim[1,3,0,(4/3,-2/3)],\\ (\nu,l)_L\ \ l=e,\mu\sim(1,1,0,-1),\quad l_R\sim(1,1,0,-2).\end{gathered} \tag{3}$$

Top-color must be broken, which we will assume is accomplished through a (effective) scalar field

$$\Phi\sim(3,\overline{3},y,-y). \tag{4}$$

When $\Phi$ develops a vacuum expectation value (VEV), it produces the simultaneous symmetry breaking:

$$\mathrm{SU}(3)_1\times\mathrm{SU}(3)_2\rightarrow\mathrm{SU}(3)_{\mathrm{QCD}}$$

and

$$\mathrm{U}(1)_{Y1}\times\mathrm{U}(1)_{Y2}\rightarrow\mathrm{U}(1)_Y. \tag{5}$$

The choice of $y$ will be specified below.

$\mathrm{SU}(3)_1\times\mathrm{U}(1)_{Y1}$ is assumed to be strong enough to form chiral condensates which will naturally be tilted in the top-quark direction by the $\mathrm{U}(1)_{Y1}$ couplings. The theory is assumed to spontaneously break down to ordinary $\mathrm{QCD}\times\mathrm{U}(1)_Y$ at a scale of $\sim 1$ TeV, before it becomes confining. The isospin splitting that permits the formation of a $\langle\overline{tt}\rangle$ condensate but disallows the $\langle\overline{bb}\rangle$ condensate is due to

the $U(1)_{Yi}$ couplings. Since they are both larger than the ordinary hypercharge gauge coupling, no significant fine-tuning is needed in principle to achieve this symmetry-breaking pattern. The $b$-quark mass in this scheme is then an interesting issue, arising from a combination of ETC effects and instantons in $SU(3)_1$. The $\theta$ term in $SU(3)_1$ may manifest itself as the $CP$-violating phase in the CKM matrix. Above all, the new spectroscopy of such a system should begin to materialize indirectly in the third generation (e.g., in $Z\to b\bar{b}$) or perhaps at the Tevatron in top and bottom quark production. The symmetry-breaking pattern outlined above will generically give rise to three (pseudo) Nambu-Goldstone bosons $\tilde{\pi}^a$, or ''top-pions,'' near the top mass scale. If the top-color scale is of the order of 1 TeV, the top pions will have a decay constant of $f_\pi \approx 50$ GeV, and a strong coupling given by a Goldberger-Treiman relation, $g_{tb\pi} \approx m_t/\sqrt{2} f_\pi \approx 2.5$, potentially observable in $\tilde{\pi}^+ \to t + \bar{b}$ if $m_{\tilde{\pi}} > m_t + m_b$.

We assume that ESB can be primarily driven by a Higgs sector or technicolor, with gauge group $G_{\rm TC}$. Technicolor can also provide condensates which generate the breaking of top-color to QCD and $U(1)_Y$, although this can also be done by a Higgs field. The coupling constants (gauge fields) of $SU(3)_1 \times SU(3)_2$ are, respectively, $h_1$ and $h_2$ ($A^A_{1\mu}$ and $A^A_{2\mu}$) while for $U(1)_{Y1} \times U(1)_{Y2}$ they are, respectively, $q_1$ and $q_2$ ($B_{1\mu}, B_{2\mu}$). The $U(1)_{Yi}$ fermion couplings are then $q_i(Yi/2)$, where $Y1, Y2$ are the charges of the fermions under $U(1)_{Y1}, U(1)_{Y2}$, respectively. A $(3,3)\times(y,-y)$ technicondensate (or Higgs boson field) breaks $SU(3)_1 \times SU(3)_2 \times U(1)_{Y1} \times U(1)_{Y2} \to SU(3)_{\rm QCD} \times U(1)_Y$ at a scale $\Lambda \gtrsim 240$ GeV, or it fully breaks $SU(3)_1 \times SU(3)_2 \times U(1)_{Y1} \times U(1)_{Y2} \times SU(2)_L \to SU(3)_{\rm QCD} \times U(1)_{\rm EM}$ at the scale $\Lambda_{\rm TC} = 240$ GeV. Either scenario typically leaves a *residual global symmetry*, $SU(3)' \times U(1)'$, implying a degenerate, massive color octet of ''colorons,'' $B^A_\mu$, and a singlet heavy $Z'_\mu$. The gluon $A^A_\mu$ and coloron $B^A_\mu$ [the SM $U(1)_Y$ field $B_\mu$ and the $U(1)'$ field $Z'_\mu$], are then defined by orthogonal rotations with mixing angle $\theta(\theta')$:

$$h_1 \sin\theta = g_3, \quad h_2 \cos\theta = g_3, \quad \cot\theta = h_1/h_2,$$

$$\frac{1}{g_3^2} = \frac{1}{h_1^2} + \frac{1}{h_2^2},$$

$$q_1 \sin\theta' = g_1, \quad q_2 \cos\theta' = g_1, \quad \cot\theta' = q_1/q_2,$$

$$\frac{1}{g_1^2} = \frac{1}{q_1^2} + \frac{1}{q_2^2}, \tag{6}$$

and $g_3$ ($g_1$) is the QCD [$U(1)_Y$] coupling constant at $\Lambda_{\rm TC}$. We ultimately demand $\cot\theta \gg 1$ and $\cot\theta' \gg 1$ to select the top-quark direction for condensation. The masses of the degenerate octet of colorons and $Z'$ are given by $M_B \approx g_3 \Lambda/\sin\theta\cos\theta$, $M_{Z'} \approx y g_1 \Lambda/\sin\theta'\cos\theta'$. The usual QCD gluonic [$U(1)_Y$ electroweak] interactions are obtained for any quarks that carry either $SU(3)_1$ or $SU(3)_2$ triplet quantum numbers [or $U(1)_{Yi}$ charges].

The coupling of the new heavy bosons $Z'$ and $B^A$ to fermions is then given by

$$\mathscr{L}_{Z'} = g_1 \cot\theta' Z' \cdot J_{Z'}, \quad \mathscr{L}_B = g_3 \cot\theta B^A \cdot J^A_B, \tag{7}$$

where the currents $J_{Z'}$ and $J_B$ in general involve all three generations of fermions:

$$J_{Z'} = J_{Z',1} + J_{Z',2} + J_{Z',3}, \quad J_B = J_{B,1} + J_{B,2} + J_{B,3}. \tag{8}$$

For the third generation the currents read explicitly (in a weak eigenbasis)

$$J^\mu_{Z',3} = \frac{1}{6}\bar{t}_L \gamma^\mu t_L + \frac{1}{6}\bar{b}_L \gamma^\mu b_L + \frac{2}{3}\bar{t}_R \gamma^\mu t_R - \frac{1}{3}\bar{b}_R \gamma^\mu b_R - \frac{1}{2}\bar{\nu}_{\tau L} \gamma^\mu \nu_{\tau L} - \frac{1}{2}\bar{\tau}_L \gamma^\mu \tau_L - \bar{\tau}_R \gamma^\mu \tau_R, \tag{9}$$

$$J^{A,\mu}_{B,3} = \bar{t}\gamma^\mu \frac{\lambda^A}{2} t + \bar{b}\gamma^\mu \frac{\lambda^A}{2} b, \tag{10}$$

where $\lambda^A$ is a Gell-Mann matrix acting on color indices. For the first two generations the expressions are similar, except for a suppression factor of $-\tan^2\theta'$ ($-\tan^2\theta$):

$$J^\mu_{Z',2} = -\tan^2\theta' \left( \frac{1}{6}\bar{c}_L \gamma^\mu c_L + \frac{1}{6}\bar{s}_L \gamma^\mu s_L + \cdots \right), \tag{11}$$

$$J^\mu_{B,2} = -\tan^2\theta \left( \bar{c}\gamma^\mu \frac{\lambda^A}{2} c + \bar{s}\gamma^\mu \frac{\lambda^A}{2} s \right), \tag{12}$$

with corresponding formulas applying to the first generation. Integrating out the heavy bosons $Z'$ and $B$, these couplings give rise to effective low-energy four-fermion interactions, which can in general be written as

$$\mathscr{L}_{{\rm eff},Z'} = -\frac{2\pi\kappa_1}{M^2_{Z'}} J_{Z'} \cdot J_{Z'}, \quad \mathscr{L}_{{\rm eff},B} = -\frac{2\pi\kappa}{M^2_B} J^A_B \cdot J^A_B, \tag{13}$$

where

$$\kappa_1 = \frac{g_1^2 \cot^2\theta'}{4\pi}, \quad \kappa = \frac{g_3^2 \cot^2\theta}{4\pi}. \tag{14}$$

The effective top-color interaction of the third generation takes the form

$$\mathscr{L}'_{\rm TopC} = -\frac{2\pi\kappa}{M^2_B} \left( \bar{t}\gamma_\mu \frac{\lambda^A}{2} t + \bar{b}\gamma_\mu \frac{\lambda^A}{2} b \right) \times \left( \bar{t}\gamma^\mu \frac{\lambda^A}{2} t + \bar{b}\gamma^\mu \frac{\lambda^A}{2} b \right). \tag{15}$$

This interaction is attractive in the color-singlet $\bar{t}t$, and $\bar{b}b$ channels and invariant under color SU(3) and $SU(2)_L \times SU(2)_R \times U(1) \times U(1)$ where $SU(2)_R$ is the custodial symmetry of the electroweak interactions.

In addition to the top-color interaction, we have the $U(1)_{Y1}$ interaction [which breaks custodial $SU(2)_R$]

$$\mathscr{L}'_{Y1} = -\frac{2\pi\kappa_1}{M_{Z'}^2}\left(\frac{1}{6}\overline{\psi_L}\gamma_\mu\psi_L + \frac{2}{3}\overline{t_R}\gamma_\mu t_R - \frac{1}{3}\overline{b_R}\gamma_\mu b_R - \frac{1}{2}\overline{l_L}\gamma_\mu l_L - \overline{\tau_R}\gamma_\mu\tau_R\right)^2, \tag{16}$$

where $\psi_L=(t,b)_L$, $l_L=(\nu_\tau,\tau)_L$, and $\kappa_1$ is assumed to be of order 1. (A small value for $\kappa_1$ would signify fine-tuning and may be phenomenologically undesirable.)

The attractive TopC interaction, for sufficiently large $\kappa$, can trigger the formation of a low-energy condensate, $\langle \overline{tt}+\overline{bb}\rangle$, which would break $SU(2)_L\times SU(2)_R \times U(1)_Y \to U(1)\times SU(2)_c$, where $SU(2)_c$ is a global custodial symmetry. On the other hand, the $U(1)_{Y1}$ force is attractive in the $\overline{tt}$ channel and repulsive in the $\overline{bb}$ channel. Thus, we can have in concert critical and subcritical values of the combinations:

$$\kappa + \frac{2\kappa_1}{9N_c} > \kappa_{\rm crit}, \quad \kappa_{\rm crit} > \kappa - \frac{\kappa_1}{9N_c}. \tag{17}$$

Here $N_c$ is the number of colors. It should be mentioned that this analysis is performed in the context of a large-$N_c$ approximation. The leading isospin-breaking effects are kept even though they are $O(1/N_c)$. The critical coupling, in this approximation, is given by $\kappa_{\rm crit}=2\pi/N_c$. In what follows, we will not make explicit the $N_c$ dependence, but rather take $N_c=3$. We would expect the cutoff for integrals in the usual Nambu–Jona-Lasinio (NJL) gap equation for $SU(3)_{\rm TopC}$ $[U(1)_{Y1}]$ to be $\sim M_B$ $(\sim M_{Z'})$. Hence, these relations define criticality conditions irrespective of $M_{Z'}/M_B$. This leads to ''tilted'' gap equations in which the top quark acquires a constituent mass, while the $b$ quark remains massless. Given that both $\kappa$ and $\kappa_1$ are large there is no particular fine-tuning occurring here, only ''rough-tuning'' of the desired tilted configuration. Of course, the NJL approximation is crude, but as long as the associated phase transitions of the real strongly coupled theory are approximately second order, analogous rough-tuning in the full theory is possible.

The full phase diagram of the model is shown in Fig. 1. The criticality conditions (17) define the allowed region in the $\kappa_1$-$\kappa$ plane in the form of the two straight solid lines intersecting at $(\kappa_1=0,\kappa=\kappa_{\rm crit})$. To the left of these lines lies the symmetric phase, in between them the region where only a $\langle\overline{tt}\rangle$ condensate forms and to the right of them the phase where both $\langle\overline{tt}\rangle$ and $\langle\overline{bb}\rangle$ condensates arise. The horizontal line marks the region above which $\kappa_1$ makes the $U(1)_{Y1}$ interaction strong enough to produce a $\langle\overline{\tau\tau}\rangle$ condensate. [This line is meant only as an indication, as the fermion-bubble (large-$N_c$) approximation, which we use, evidently fails for leptons.] There is an additional constraint from the measurement of $\Gamma(Z\to\tau^+\tau^-)$, confining the allowed region to the one below the solid curve. This curve corresponds to a $2\sigma$ discrepancy between the top-color prediction (computed to lowest nontrivial order in the coupling $\kappa_1$) and the measured value of this width. Note that the known value of the top quark mass determines the cutoff $M_B$ in terms of $\kappa$ and $\kappa_1$. This is illustrated by the slanted lines which represent

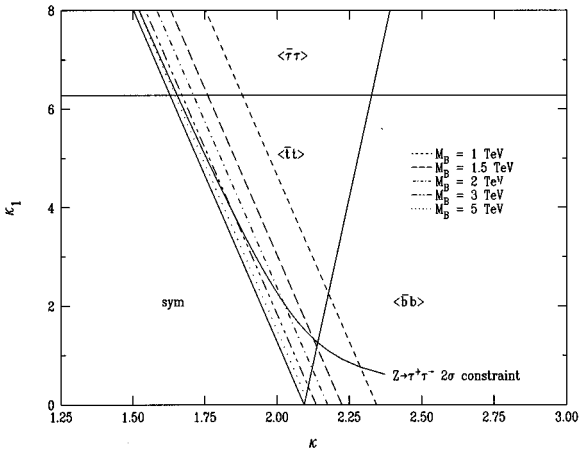


FIG. 1. Phase diagram of the top-color model I discussed in Sec. II A.

curves of constant $M_B$. In this figure, the $Z'$ boson mass is taken to be equal to $M_B$. In the allowed region a top condensate alone forms. The constraints favor a strong $SU(3)_{\rm TopC}$ coupling and a relatively weaker $U(1)_{Y1}$ coupling.

We note that recently Appelquist and Evans have proposed a scheme in which the tilting interaction is a non-Abelian gauge group, rather than a U(1) [13]. This has the advantage of asymptotic freedom in the tilting interaction immediately above the scale of TopC condensation.

### B. Anomaly-free model without a strong U(1) (top-color II)

The strong U(1) is present in the previous scheme to avoid a degenerate $\langle\overline{tt}\rangle$ with $\langle\overline{bb}\rangle$. However, we can give a model in which there is (i) a top-color SU(3) group but (ii) no strong U(1) with (iii) an anomaly-free representation content. In fact the original model of [5] was of this form, introducing a new quark of charge $-1/3$. Let us consider a generalization of this scheme which consists of the gauge structure $SU(3)_Q\times SU(3)_1\times SU(3)_2\times U(1)_Y\times SU(2)_L$. We require an additional triplet of fermion fields $(Q_R^a)$ transforming as (3,3,1) and $Q_L^a$ transforming as (3,1,3) under the $SU(3)_Q\times SU(3)_1\times SU(3)_2$.

The fermions are then assigned the following quantum numbers in $SU(2)\times SU(3)_Q\times SU(3)_1\times SU(3)_2\times U(1)_Y$:

$$(t,b)_L \ \ (c,s)_L \sim (2,1,3,3), \quad Y=1/3, \tag{18}$$

$$(t)_R \sim (1,1,3,3), \quad Y=4/3,$$

$$(Q)_R \sim (1,3,3,1), \quad Y=0,$$

$$(u,d)_L \sim (2,1,1,3), \quad Y=1/3,$$

$$(u,d)_R \ \ (c,s)_R \sim (1,1,1,3), \quad Y=(4/3,-2/3),$$

$$(\nu,l)_L \ \ l=e,\mu,\tau \sim (2,1,1,1), \quad Y=-1,$$

$$(l)_R \sim (1,1,1,1), \quad Y=-2,$$

$$b_R \sim (1,1,1,3), \quad Y=2/3,$$

$$(Q)_L \sim (1,3,1,3), \quad Y=0.$$

Thus, the $Q$ fields are electrically neutral. One can verify that this assignment is anomaly free.

The $SU(3)_Q$ confines and forms a $\langle \overline{Q}Q \rangle$ condensate which acts like the $\Phi$ field and breaks the top-color group down to QCD dynamically. We assume that $Q$ is then decoupled from the low-energy spectrum by its large constituent mass. There is only a lone U(1) Nambu-Goldstone boson $\sim \overline{Q}\gamma^5 Q$ which acquires a large mass by $SU(3)_Q$ instantons.

The $SU(3)_1$ is chiral-critical, and a condensate forms which defines the $\langle \overline{tt} \rangle$ direction spontaneously. If we turn off the $SU(2)\times U(1)_Y$ and Higgs-Yukawa couplings, then the strongly coupled $SU(3)_1$ sector has an $SU(4)_L \times U(1)_R \times U(1)_L$ global chiral symmetry. Let us define $\Psi_L=(t,b,c,s)_L$. The effect of $SU(3)_1$ after integrating out the massive colorons and $Q$ fields is a strong four-fermion, NJL-like interaction of the form

$$\begin{aligned} G(\overline{\Psi_L^i} t_R)(\overline{t_R}\Psi_{Li}) &\to (\overline{\Psi_L^i} t_R F_i + \text{ H.c.}) - G^{-1} F^\dagger F \\ &= [(\overline{T_L^i} t_R) H_i + (\overline{C_L^i} t_R) K_i + \text{H.c.}] \\ &\quad - G^{-1}(H^\dagger H + K^\dagger K), \end{aligned} \tag{19}$$

where we indicate the factorization into a composite field quadruplet under $SU(4)_L$, $F^i$. We further decompose $F$ into doublets $F=(H,K)$. By definition, $H$ acquires a VEV giving the top mass, while the remaining components of $H$ are a massive neutral Higgs-like $\sigma$ boson, and a triplet of top-pions as before. Here the novelty is that $K$ will be, at this stage, a completely massless set of NGB's, ''charm-top-pions.'' When $SU(2)_L \times U(1)$ and the Yukawa interactions to the effective Higgs field are switched on, the top-pions and charm-top-pions all become massive. These will then mediate strong interactions, but which are distinctly nonleptonic in the present scheme. We discuss their phenomenological consequences, mainly for $D^0$-$\overline{D^0}$ mixing, in Sec. IV B.

### C. Triangular textures

The texture of the fermion mass matrices will generally be controlled by the symmetry breaking pattern of a horizontal symmetry. In the present case we are specifying a residual top-color symmetry, presumably subsequently to some initial breaking at some scale $\Lambda$, large compared to top-color, e.g., the third-generation fermions in model I have different top-color assignments than do the second- and first-generation fermions. Thus the texture will depend in some way upon the breaking of top-color.

Let us study a fundamental Higgs boson, which ultimately breaks $SU(2)_L \times U(1)_Y$, together with an effective field $\Phi$ breaking top-color as in Eq. (5). We must now specify the full top-color charges of these fields. As an example, under $SU(3)_1 \times SU(3)_2 \times U(1)_{Y1} \times U(1)_{Y2} \times SU(2)_L$ let us choose

$$\Phi \sim (3,\overline{3},\tfrac{1}{3},-\tfrac{1}{3},0), \quad H \sim (1,1,0,-1,\tfrac{1}{2}). \tag{20}$$

The effective couplings to fermions that generate mass terms in the up sector are of the form

$$\begin{aligned} -\mathscr{L}_{\mathscr{M}_U} &= m_0 \overline{t_L} t_R + c_{33} \overline{T_L} t_R H \frac{\det\Phi^\dagger}{\Lambda^3} + c_{32} \overline{T_L} c_R H \frac{\Phi}{\Lambda} \\ &\quad + c_{31} \overline{T_L} u_R H \frac{\Phi}{\Lambda} + c_{23} \overline{C_L} t_R H \Phi^\dagger \frac{\det\Phi^\dagger}{\Lambda^4} \\ &\quad + c_{22} \overline{C_L} c_R H + c_{21} \overline{C_L} u_R H + c_{13} \overline{F_L} t_R H \Phi^\dagger \frac{\det\Phi^\dagger}{\Lambda^4} \\ &\quad + c_{12} \overline{F_L} c_R H + c_{11} \overline{F_L} u_R H + \text{H.c.} \end{aligned} \tag{21}$$

Here $T=(t,b)$, $C=(c,s)$, and $F=(u,d)$. The mass $m_0$ is the dynamical condensate top mass. Furthermore, $\det\Phi$ is defined by

$$\det\Phi \equiv \frac{1}{6} \epsilon_{ijk} \epsilon_{lmn} \Phi_{il} \Phi_{jm} \Phi_{kn}, \tag{22}$$

where in $\Phi_{rs}$ the first [second] index refers to $SU(3)_1$ [$SU(3)_2$]. The matrix elements now require factors of $\Phi$ to connect the third- with the first- or second-generation color indices. The down quark and lepton mass matrices are generated by couplings analogous to (21).

To see what kinds of textures can arise naturally, let us assume that the ratio $\Phi/\Lambda$ is small, $O(\epsilon)$. The field $H$ acquires a VEV of $v$. Then the resulting mass matrix is approximately triangular:

$$\begin{pmatrix} c_{11}v & c_{12}v & \sim 0 \\ c_{21}v & c_{22}v & \sim 0 \\ c_{31}O(\epsilon)v & c_{32}O(\epsilon)v & \sim m_0 + O(\epsilon^3)v \end{pmatrix}, \tag{23}$$

where we have kept only terms of $O(\epsilon)$ or larger.

This is a triangular matrix (up to the $c_{12}$ term). When it is written in the form $U_L \mathscr{D} U_R^\dagger$ with $U_L$ and $U_R$ unitary and $\mathscr{D}$ positive diagonal, there automatically result restrictions on $U_L$ and $U_R$. In the present case, the elements $U_L^{3,i}$ and $U_L^{i,3}$ are vanishing for $i \neq 3$, while the elements of $U_R$ are not constrained by triangularity. Analogously, in the down quark sector $D_L^{i,3} = D_L^{3,i} = 0$ for $i \neq 3$ with $D_R$ unrestricted. The situation is reversed when the opposite corner elements are small, which can be achieved by choosing $H \sim (1,1,-1,0,1/2)$.

These restrictions on the quark rotation matrices have important phenomenological consequences. For instance, in the process $B^0 \to \overline{B^0}$ there are potentially large contributions from top-pion and coloron exchange. However, as we show in Sec. IV B, these contributions are proportional to the product $D_L^{3,1} D_R^{3,1}$. The same occurs in $D^0$-$\overline{D^0}$ mixing, where the effect goes as products involving $U_L$ and $U_R$ off-diagonal elements. Therefore, triangularity can naturally select these products to be small.

Selection rules will be a general consequence in models where the generations have different gauge quantum numbers above some scale. The precise selection rules depend upon the particular symmetry breaking that occurs. This example is merely illustrative of the systematic effects that can occur in such schemes.

## III. EFFECTIVE LAGRANGIAN ANALYSIS

### A. Low-energy theory

Let us study a standard model Higgs boson together with an effective Nambu–Jona-Lasinio [14] mechanism arising from the interactions of Eqs. (15) and (16). The standard model Higgs boson $H$ is used presently to simulate the effects of TC, and its small Yukawa couplings to the top and bottom quarks simulate the effects of ETC. In addition, the four-fermion interaction is introduced to simulate the effects of TopC (model I).

We can conveniently treat the dynamics of this combined system using the renormalization group by writing a Yukawa form of the four-fermion interactions, as defined at the cutoff scale $\Lambda$, with the help of a static auxiliary Higgs field.

At the starting point we will have three bound-state doublets: an ordinary Higgs boson $H$ whose VEV drives electroweak symmetry breaking, a doublet $\phi_1$ whose VEV mainly gives a large mass to the top and another doublet $\phi_2$ coupling mainly to bottom [11]. The effective Lagrangian at the cutoff $\Lambda$ (identified with $M_B \approx M_{Z'}$ of Sec. II A) is

$$\begin{aligned}\mathscr{L} = {} & \overline{\Psi}_L^{(3)} \phi_1 t_R + \overline{\Psi}_L^{(3)} \phi_2 b_R + \kappa' \Lambda^2 e^{i\theta} \det(\phi_1 \phi_2) + \text{H.c.} \\ & - \Lambda_1^2 \phi_1^\dagger \phi_1 - \Lambda_2^2 \phi_2^\dagger \phi_2 + D_\mu H^\dagger D^\mu H - M_H^2 H^\dagger H \\ & - \frac{\lambda}{2} (H^\dagger H)^2 + [\epsilon_U^{ij} \overline{\Psi}_L^i H U_R^j + \epsilon_D^{ij} \overline{\Psi}_L^i H^c D_R^j + \text{H.c.}] \\ & + \mathscr{L}_{\text{gauge}}, \end{aligned} \tag{24}$$

where $\overline{\Psi}_L, U_R, D_R$ have the obvious meaning; $\mathscr{L}_{\text{gauge}}$ contains the gauge and fermion kinetic terms; and $\Lambda_{1,2}^2 = \Lambda^2/\lambda_{1,2}^2$ satisfy $\Lambda_2 > \Lambda_1$, with

$$\lambda_1^2 = 4\pi\left(\kappa + \frac{2\kappa_1}{27}\right), \quad \lambda_2^2 = 4\pi\left(\kappa - \frac{\kappa_1}{27}\right). \tag{25}$$

The parameters $\kappa$ and $\kappa_1$ were defined in Sec. II A. In (24), $i,j$ are generation indices. The determinant term in the expression for the effective Lagrangian arises from top-color instantons, and $\theta$ is the strong top-color $CP$ phase. This term is a bosonized form of a 't Hooft flavor determinant $k e^{i\theta} \det(\overline{\Psi}_L^{(3)} \Psi_R^{(3)})/\Lambda^2$, where the constant $k$ is expected to be $O(1)$. These effects are similar to those in QCD that elevate the $\eta'$ mass; we assume the QCD $CP$ phase is zeroed by, e.g., an exact Peccei-Quinn symmetry. Presently, the top-color $\theta$ angle will provide an origin for CKM $CP$ violation. The coefficient $\kappa'$ is related to $k$ through

$$\kappa' = \frac{k}{\lambda_1^2 \lambda_2^2} \tag{26}$$

and is thus small, as are the matrices $\epsilon_{U,D}$. We shall write

$$\epsilon_{U,D}^{ij} = \epsilon \eta_{U,D}^{ij}, \quad \kappa' = -\epsilon \eta_k \tag{27}$$

and treat $\epsilon$ as small compared to unity. The $\epsilon_{U,D}^{ij}$ will reflect the textures as considered in Sec. II C. The $\eta$'s are then $O(1)$. Equation (24) will be the starting point of our investigations.

We now integrate out degrees of freedom with momenta between a scale $\mu$ and the cutoff $\Lambda$. This calculation is performed in the large-$N_c$ limit and cutting off the fermion loops at $\Lambda$. The effective Lagrangian at the scale $\mu$ has the form

$$\begin{aligned}\mathscr{L} = {} & \mathscr{L}_{\text{gauge}} + D_\mu H^\dagger D^\mu H - M_H^2 H^\dagger H - \frac{\lambda}{2} (H^\dagger H)^2 \\ & + Z\ \text{tr} D_\mu \Sigma^\dagger D^\mu \Sigma - \Lambda_1^2 \phi_1^\dagger \phi_1 - \Lambda_2^2 \phi_2^\dagger \phi_2 \\ & + \frac{3}{8\pi^2} (\Lambda^2 - \mu^2) \text{tr} \Sigma^\dagger \Sigma - \frac{3}{16\pi^2} \ln(\Lambda^2/\mu^2) \text{tr}(\Sigma^\dagger \Sigma)^2 \\ & + [\overline{\Psi}_L^i \Sigma^{ij} \Psi_R^j + \text{H.c.}] + [\kappa' \Lambda^2 e^{i\theta} \det(\phi_1 \phi_2) + \text{H.c.}], \end{aligned} \tag{28}$$

where the $\Sigma^{ij}$ are matrices

$$\Sigma^{ij} = (\phi_1 \delta^{i3} \delta^{j3} + \epsilon_U^{ij} H, \phi_2 \delta^{i3} \delta^{j3} + \epsilon_D^{ij} H^c), \tag{29}$$

and the trace is taken over both generation and SU(2) indices. The constant $Z$ is given by

$$Z = \frac{3}{16\pi^2} \ln(\Lambda^2/\mu^2). \tag{30}$$

The mixing between $H$ and $\phi_1, \phi_2$ involves only $\epsilon_{U,D}^{33}$ to first order in $\epsilon$. So, for the scalar potential, we disregard the Higgs couplings to the first two generations and simplify $\Sigma$ into a $2 \times 2$ matrix

$$\Sigma = (\phi_1 + \epsilon \eta_t H, \phi_2 + \epsilon \eta_b H^c). \tag{31}$$

It is convenient to write $V$ in terms of $H$ and $\Sigma$ rather than $H$ and $\phi_i$. To $O(\epsilon)$, we may also substitute $\det\Sigma$ for $\det(\phi_1, \phi_2)$. Writing $F \equiv 3/(8\pi^2)$ and dropping $\mu^2$ compared to $\Lambda^2$, we have the potential

$$\begin{aligned} V = {} & M_H^2 H^\dagger H + \frac{\lambda}{2} (H^\dagger H)^2 + \Lambda_1^2 \Sigma_{i1}^* \Sigma_{i1} + \Lambda_2^2 \Sigma_{i2}^* \Sigma_{i2} \\ & - F\Lambda^2 \text{tr} \Sigma^\dagger \Sigma + Z \text{tr}(\Sigma^\dagger \Sigma)^2 + [-\epsilon \Lambda_1^2 \eta_t \Sigma_{i1}^* H_i \\ & + \epsilon \Lambda_2^2 \eta_b \epsilon_{ij} \Sigma_{i2}^* H_j^* + \epsilon \eta_k \Lambda^2 e^{i\theta} \det\Sigma + \text{H.c.}], \end{aligned} \tag{32}$$

where $\Sigma_{i1}$ is the first column of $\Sigma$ so that $\phi_{1i} = \Sigma_{i1} - \epsilon \eta_t H_i$, etc. Note $H_i^c = -\epsilon_{ij} H_j^*$. Without loss of generality we can take $\eta_t$ real and positive by appropriately choosing the phase of the field $H$. The phase of $\eta_b$ can be absorbed in $\theta$ by an appropriate rotation of $b_R$.

To $O(\epsilon^0)$ the minimum of the potential is determined by

$$\begin{aligned} \langle H^\dagger H \rangle \equiv v_0^2 = -\frac{M_H^2}{\lambda}, \\ \langle \Sigma_{i1}^* \Sigma_{i1} \rangle \equiv f_0^2 = \langle \phi_1^\dagger \phi_1 \rangle, \\ \langle \Sigma_{i2}^* \Sigma_{i2} \rangle = 0, \end{aligned} \tag{33}$$

where $f_0$ satisfies the equation

$$\Lambda_1^2 - F\Lambda^2 + F f_0^2 \ln(\Lambda^2/\mu^2) = 0 \tag{34}$$

and the last condition in Eq. (33) results from the assumption that $\Lambda_2^2 - F\Lambda^2 > 0$. We can work out the minimization of the potential to $O(\epsilon)$. We find

$$\langle H\rangle = \begin{pmatrix} v_0 + \epsilon v_1 \\ 0 \end{pmatrix}, \quad \langle \Sigma\rangle = \begin{pmatrix} f_0 + \epsilon f_1 & 0 \\ 0 & \epsilon f_2 \end{pmatrix}, \tag{35}$$

where

$$\mathrm{Re}v_1 = \frac{\Lambda_1^2 \eta_t f_0}{2\lambda v_0^2}, \tag{36}$$

$$\mathrm{Im}v_1 = \frac{v_0}{\Lambda_1^2 \eta_t f_0} \mathrm{Im}(\eta_b \eta_k \Lambda^2 f_0 e^{i\theta} + \Lambda_2^2 \eta_b f_2^*), \tag{37}$$

$$f_1 = \frac{\Lambda_1^2 \eta_t v_0}{4Z f_0^2}, \tag{38}$$

$$f_2 = \frac{\Lambda_2^2 \eta_b v_0 - \Lambda^2 \eta_k e^{-i\theta} f_0}{\Lambda_2^2 - F\Lambda^2}. \tag{39}$$

Here we have performed an SU(2)×U(1) rotation to make $\Sigma_{11}$ real and $\Sigma_{21}$ equal to zero. Note, in particular, that the vacuum aligns properly, provided $\eta_t \neq 0$. This statement is in fact true to all orders in $\epsilon$. Furthermore, if we ignore mixing with the first two generations, the top and bottom quark masses are given by

$$m_t = |f_0 + \epsilon f_1|, \tag{40}$$

$$m_b = \epsilon |f_2|. \tag{41}$$

Note that the denominator in Eq. (39) can be small, thus enhancing the size of the $b$-quark mass [11].

In order to obtain expressions for the scalar and pseudoscalar masses we must diagonalize the potential in (32). Let $\chi_i'$ denote the two columns of $\Sigma$ and define

$$\chi_1 = \sqrt{Z}\chi_1', \quad \chi_2 = \sqrt{Z}\chi_2'^c. \tag{42}$$

Then the kinetic term for the scalars is simply

$$\mathscr{L}_{\mathrm{kin}} = D_\mu H^\dagger D^\mu H + D_\mu \chi_1^\dagger D^\mu \chi_1 + D_\mu \chi_2^\dagger D^\mu \chi_2 \tag{43}$$

and the potential reads

$$\begin{aligned} V = {} & M_H^2 H^\dagger H + Z^{-1}(\Lambda_1^2 - F\Lambda^2)\chi_1^\dagger \chi_1 \\ & + Z^{-1}(\Lambda_2^2 - F\Lambda^2)\chi_2^\dagger \chi_2 - \epsilon \Lambda_1^2 Z^{-1/2} \eta_t (\chi_1^\dagger H + H^\dagger \chi_1) \\ & + \epsilon \Lambda_2^2 Z^{-1/2} \eta_b (\chi_2^\dagger H + H^\dagger \chi_2) - \epsilon \Lambda^2 Z^{-1} \\ & \times \eta_k (e^{-i\theta} \chi_1^\dagger \chi_2 + \mathrm{H.c.}) + \frac{\lambda}{2}(H^\dagger H)^2 + Z^{-1}[(\chi_1^\dagger \chi_1)^2 \\ & + (\chi_2^\dagger \chi_2)^2 + 2(\chi_1^\dagger \chi_1)(\chi_2^\dagger \chi_2) - 2(\chi_1^\dagger \chi_2)(\chi_2^\dagger \chi_1)]. \end{aligned} \tag{44}$$

The VEV's of the fields $H, \chi_1$ and $\chi_2$ add in quadrature to give the electroweak scale (so, for example, to lowest order $v_w = \sqrt{v_0^2 + Z f_0^2} = 174$ GeV). We diagonalize the potential to obtain the mass eigenstates. In the charged sector we find, apart from the Goldstone bosons $w^\pm$ of electroweak symmetry breaking, a pair of (complex-conjugate) pseudo Goldstone bosons (the top-pions) of mass

$$m_{\tilde{\pi}^\pm}^2 = \epsilon \Lambda_1^2 \eta_t \left( \frac{v_0}{Z f_0} + \frac{f_0}{v_0} \right) \tag{45}$$

(in agreement with expectations from, e.g., current algebra) and a pair of massive states

$$m_{\tilde{H}^\pm}^2 = Z^{-1}(\Lambda_2^2 - F\Lambda^2 + 2Z f_0^2) + \epsilon \Lambda_1^2 \eta_t \frac{v_0}{Z f_0}. \tag{46}$$

The charged components of the doublets $H$ and $\chi_1$ mix with an angle

$$\phi = \arctan(Z^{1/2} f_0 / v_0) \tag{47}$$

to produce the mass eigenstates $w^\pm$ and $\tilde{\pi}^\pm$ (recall $Z^{1/2} f_0$ is the top-pion ''decay constant''). There are further mixings at $O(\epsilon)$ among all three doublets, which are also easily calculable. They will determine some of the couplings of fermions to scalars which do not occur at leading order (e.g., top-pion couplings to $b_R$ or $\tilde{H}^\pm$ couplings to $t_R$).

In the neutral sector we find the following eigenvalues:

$$\begin{aligned} & m_z^2 = 0, \quad \text{Goldstone boson}, \\ & m_{\tilde{\pi}^0}^2 = \epsilon \Lambda_1^2 \eta_t \left( \frac{v_0}{Z f_0} + \frac{f_0}{v_0} \right), \quad \text{neutral top-pion}, \\ & m_A^2 = Z^{-1}(\Lambda_2^2 - F\Lambda^2), \quad \text{bound state } \overline{b}\gamma^5 b, \\ & m_{\tilde{H}^0}^2 = Z^{-1}(\Lambda_2^2 - F\Lambda^2), \quad \text{bound state } \overline{bb}, \\ & m_{h_1}^2 = 2\lambda v_0^2 + O(\epsilon), \quad \text{standard Higgs boson}, \\ & m_{h_2}^2 = 4 f_0^2 + O(\epsilon), \quad \text{top-quark–Higgs-boson}. \end{aligned} \tag{48}$$

To leading order, the only mixing occurs between the imaginary parts of the neutral components of $H$ and $\chi_1$, the mixing angle is the same as in the case of the charged sector, as expected. There are further mixings at $O(\epsilon)$. Because of the $CP$-violating angle $\theta$ there are mixings between $CP$-even and $CP$-odd fields.

### B. Fermion mass matrices and mixings

We will now determine whether this low-energy structure gives rise to realistic quark mixings and weak $CP$ violation. Consider first the mass matrix in the top sector:

$$-\mathscr{M}_U^{ij} = f_t \delta^{i3} \delta^{j3} + \epsilon \eta_U^{ij} v_0, \tag{49}$$

where $|f_t| \approx m_t$. This is diagonalized by unitary matrices $U_L$ and $U_R$ such that

$$U_L^\dagger \mathscr{M}_U U_R = \mathscr{D}, \tag{50}$$

where $\mathscr{D} = \mathrm{diag}(m_u, m_c, m_t)$. The matrix $U_L$ has then the approximate form

$$U_L=\begin{pmatrix} \cos\phi & -\sin\phi & \epsilon\beta \\ \sin\phi & \cos\phi & \epsilon\beta' \\ -\epsilon(\beta^*\cos\phi+\beta'^*\sin\phi) & \epsilon(\beta^*\sin\phi-\beta'^*\cos\phi) & 1 \end{pmatrix}, \tag{51}$$

where $\phi$ is of order 1 and

$$\epsilon\beta=\epsilon\frac{v_0\eta_U^{13}}{f_t}, \tag{52}$$

$$\epsilon\beta'=\epsilon\frac{v_0\eta_U^{23}}{f_t}. \tag{53}$$

Since the matrix $\eta_U$ determines the masses of the lower generation up-type quarks, we expect $\epsilon v_0\eta_U^{j3}\sim m_c$. Hence $\epsilon\beta,\epsilon\beta'=O(m_c/m_t)$. Similarly, in the bottom sector, the mass matrix is

$$-\mathscr{M}_D^{ij}=f_b\delta^{i3}\delta^{j3}+\epsilon\eta_D^{ij}v_0, \tag{54}$$

where $f_b=\langle\phi_2\rangle_2$. In principle, $f_b$ is of order $\epsilon$, but we will assume that the instanton or enhancement effects are large enough to account for the large $b$-quark mass relative to that of the other charge $-1/3$ quarks [see the remark following Eq. (41)]. That is, we assume that $f_b\gg\epsilon v_0\eta_D^{ij}$. We obtain, as above, the corresponding unitary matrix $D_L$. Note the following: (i) we can perform an arbitrary rotation in the space of the $d$ and $s$ quarks to make the corresponding angle $\phi$ [cf. Eq. (51)] equal to zero; (ii) we would like to investigate whether the angle $\theta$ can be the sole source of weak $CP$ violation. Hence we would like to take the matrices $\eta_U,\eta_D$ to be real. Then the matrix $U_L$ above is real, but $D_L$ is not, because $f_b$ is complex [see Eq. (39)]. The matrix $D_L$ then has the form

$$D_L=\begin{pmatrix} 1 & 0 & \alpha e^{i\delta} \\ 0 & 1 & \alpha' e^{i\delta} \\ -\alpha e^{-i\delta} & -\alpha' e^{-i\delta} & 1 \end{pmatrix}, \tag{55}$$

where $\alpha,\alpha'$ are real (and small),

$$\alpha=\epsilon\frac{v_0\eta_D^{13}}{|f_b|},\quad \alpha'=\epsilon\frac{v_0\eta_D^{23}}{|f_b|}, \tag{56}$$

and the angle $\delta$ can be of order 1:

$$\tan\delta=\tan\,\mathrm{Arg}f_b^*\approx\frac{-\Lambda^2\eta_k f_0\sin\theta}{\Lambda_2^2\eta_b v_0-\Lambda^2\eta_k f_0\cos\theta}. \tag{57}$$

If the instanton effects are dominant, then $|\delta|\approx|\theta|$. Note that, since the matrix $\eta_D$ determines the down- and strange-quark masses, we expect $\alpha,\alpha'=O(m_s/m_b)$, as $|f_b|\approx m_b$. So $\alpha,\alpha'$ are expected to be larger than the corresponding elements $(\epsilon\beta,\epsilon\beta')$ of $U_L$.

The Kobayashi-Maskawa matrix $V\equiv U_L^\dagger D_L$ now reads

$$V=\begin{pmatrix} c_\phi+O(\epsilon) & s_\phi+O(\epsilon) & c_\phi(\alpha e^{i\delta}-\epsilon\beta)+s_\phi(\alpha' e^{i\delta}-\epsilon\beta') \\ -s_\phi+O(\epsilon) & c_\phi+O(\epsilon) & c_\phi(\alpha' e^{i\delta}-\epsilon\beta')-s_\phi(\alpha e^{i\delta}-\epsilon\beta) \\ -\alpha e^{-i\delta}+\epsilon\beta & -\alpha' e^{-i\delta}+\epsilon\beta' & 1 \end{pmatrix}, \tag{58}$$

where $c_\phi\equiv\cos\phi$, $s_\phi\equiv\sin\phi$. This successfully predicts $|V_{cb}|\approx|V_{ts}|\approx m_s/m_b$, but does not distinguish between the first two generations, given that we do not incorporate any dynamics to do so. The $\eta$ matrices will have to be such as to suppress $\alpha$ and give $\phi\approx\theta_c$, the Cabibbo angle. A certain cancellation will still have to occur between the two terms in $V_{ub}$ in order to bring it to the correct value. We also note that, with $\epsilon\beta\sim m_c/m_t$, $\alpha'\sim m_s/m_b$ and $\alpha$ small, one obtains a Jarlskog parameter of the right size: $J\approx-\epsilon\beta\alpha'\sin\phi\cos\phi\sin\delta\sim 6\times10^{-5}\sin\delta$.

## IV. LOW-ENERGY PHENOMENOLOGY

In this section we study some of the consequences of top-color dynamics in low-energy processes. Potentially large flavor-changing neutral currents (FCNC's) arise when the quark fields are rotated from their weak eigenbasis to their mass eigenbasis. In the case of model I, the presence of a residual U(1) interacting strongly with the third generation implies that the $Z'$ will also couple to leptons in order to cancel anomalies. This generates contributions to a number of semileptonic processes. On the other hand, in model II the induced four-fermion interactions remain nonleptonic. In all cases where quark field rotations are involved we must choose an ansatz for the mass matrices or, equivalently, for $U_{L,R}$ and $D_{L,R}$ as defined in previous sections.

A possible choice is to take the square root of the CKM matrix as an indication of the order of magnitude of the effects. This is compatible with the matrices derived in (51) and (55), regarding the mixing of the third and the second generations. However, this simple ansatz does not make a distinction between the left- and the right-handed couplings. Such a distinction might arise in some realizations of the models, as seen in Sec. II C where triangular textures were derived. In those cases, the vanishing of some of the off-diagonal elements precludes contributions to particle-

antiparticle mixing from nonleptonic four-fermion interactions, although they do not have the same effect in semileptonic transitions, where left and right mixing factors enter additively rather than multiplicatively. We first present the constraints on top-color FCNC from the existing data on $b\to s\gamma$ as well as $B^0-\overline{B^0}$ and $D^0-\overline{D^0}$ mixing. Then we show several predictions for semileptonic processes.

### A. Constraints from $b\to s\gamma$

The recent measurement of the inclusive branching ratio for the process $b\to s\gamma$ [15], puts severe constraints on a variety of extensions of the standard model (SM) [16]. We study here the constraints on top-color models. In doing so we will neglect possible long-distance contributions to the $b\to s\gamma$ rate. Long-distance effects have been estimated in the literature [17] to be somewhere between 5 and 50 % of the rate and would loosen these constraints.

The effective Hamiltonian for $b\to s\gamma$ transitions is given by [18–20]

$$H_{\rm eff}=-\frac{4}{\sqrt{2}}G_F V_{ts}^* V_{tb}\sum_i C_i(\mu)O_i(\mu). \tag{59}$$

At the weak scale, the only contributing operator is

$$O_7=\frac{e}{16\pi^2}m_b(\overline{s}\sigma_{\mu\nu}b_R)F^{\mu\nu}. \tag{60}$$

However, when evolving down to the low-energy scale $\mu\simeq m_b$, $O_7$ will mix with the gluonic penguin operator

$$O_8=\frac{g}{16\pi^2}m_b(\overline{s_\alpha}\sigma_{\mu\nu}T^a_{\alpha\beta}b_{R\beta})G_a^{\mu\nu}, \tag{61}$$

as well as with the four-quark operators $O_1$–$O_6$ [18–20].

The top-color I contributions to $C_7(M_W)$ have been previously considered in [6,11]. They arise from the couplings of $\phi_1$ and $\phi_2$ to quarks in (24). Their charged components, the top pion $\widetilde{\pi}^+$ and the charged scalar $\widetilde{H}^+$, give additional penguin diagrams where they replace the $W$. They also generate contributions to the new operators $O_7'$ and $O_8'$ that are obtained by switching the chirality of quarks in (60) and (61). If one neglects the running from the top-pion and $\widetilde{H}^+$ mass scales down to $M_W$, the coefficients of $O_7$ and $O_7'$ now take the form [11]

$$C_7(M_W)=-\frac{1}{2}A(x_W)+\frac{D_L^{bs*}}{V_{ts}^*}\left(\frac{v_w}{f_{\widetilde{\pi}}}\right)^2\times\left[\frac{m_b^*}{m_b}[B(x_{\widetilde{\pi}^\pm})-B(x_{\widetilde{H}^\pm})]-\frac{1}{6}A(x_{\widetilde{\pi}^\pm})\right], \tag{62}$$

$$C_7'(M_W)=-\frac{D_R^{bs*}}{V_{ts}^*}\left(\frac{v_w}{f_{\widetilde{\pi}}}\right)^2\times\left[\frac{1}{6}A(x_{\widetilde{H}^\pm})-\frac{m_b^*}{m_b}[B(x_{\widetilde{\pi}^\pm})-B(x_{\widetilde{H}^\pm})]\right], \tag{63}$$

where $x_i=m_t^2/m_i^2$ and the functions $A(x)$ and $B(x)$ are given in [18]. Here $D_L$ and $D_R$ are the matrices defining the rotation from the weak to the mass eigenbasis in the down sector, defined in a way analogous to Eq. (50) for the up sector, and $f_{\widetilde{\pi}}\sim 50$ GeV is the top-pion decay constant. The parameter $m_b^*$ is proportional to the couplings of $\phi_1$ to $b_R$ and $\phi_2$ to $t_R$ which are only induced by instantons and mixing effects. For definiteness, we shall assume that the $b$ quark mass is mainly generated by the instanton dynamics, with a piece of $\sim 1$ GeV coming from the explicit Higgs Yukawa coupling. These two effects add with an unknown sign, so, under our assumptions, the ratio $m_b^*/m_b$ lies in the range $0.8\lesssim m_b^*/m_b\lesssim 1.2$. We have used the value 0.8 in our numerical estimates. Variation of $m_b^*/m_b$ in the above range tends to tighten the constraints we report, but not substantially.

In order to account for the renormalization-group evolution of $C_7$ and $C_7'$ down to the low-energy scale we need to know also the coefficients of $O_8$ and $O_8'$, including top-color contributions. At the $M_W$ scale these coefficients, $C_8(M_W)$ and $C_8'(M_W)$, can be obtained from $C_7(M_W)$ and $C_7'(M_W)$ by simply replacing $A\to D$ and $B\to E$, where the functions $D(x)$ and $E(x)$ are also defined in [18]. At the scale $\mu\simeq m_b$, $O_7$ mixes with $O_8$ as well as with the four-quark operators. The complete leading logarithmic approximation, within the SM first obtained in [19], gives

$$C_7(m_b)=\eta^{16/23}C_7(M_W)+\frac{8}{3}(\eta^{14/23}-\eta^{16/23})C_8(M_W)+\sum_{i=1}^{8}h_i\eta^{p_i}, \tag{64}$$

where $\eta=\alpha_s(M_W)/\alpha_s(m_b)$. The coefficients $h_i$ and $p_i$ can be found in [20]. The ''wrong'' chirality operator $O_7'$ mixes exclusively with $O_8'$, giving

$$C_7'(m_b)=\eta^{16/23}C_7'(M_W)+\frac{8}{3}(\eta^{14/23}-\eta^{16/23})C_8'(M_W). \tag{65}$$

The current experimental information on the inclusive $b\to s\gamma$ rate comes from the recent CLEO measurement [15], $B(b\to s\gamma)=(2.32\pm 0.57\pm 0.35)\times 10^{-4}$ which can be translated into 95% confidence level upper and lower limits as

$$1\times 10^{-4}<B(b\to s\gamma)<4.2\times 10^{-4}. \tag{66}$$

Normalized by the inclusive semileptonic branching ratio, the $b\to s\gamma$ branching fraction can be written as

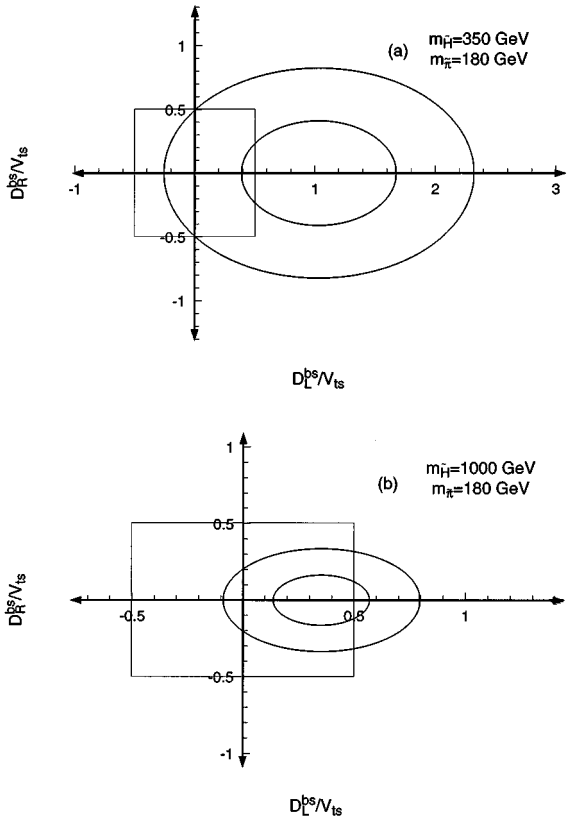


FIG. 2. Constraints from $b\to s\gamma$ in the $(D_L^{bs}/V_{ts}, D_R^{bs}/V_{ts})$ plane. Here $D_L^{bs}/V_{ts}$ is assumed to be real. The allowed region between the two ellipses corresponds to the 95% C.L. lower and upper bounds from Ref. [15]. (a) is for $m_{\tilde{H}^\pm}=350$ GeV, whereas (b) is for $m_{\tilde{H}^\pm}=1000$ GeV. In both cases, $m_{\tilde{\pi}^\pm}=180$ GeV.

$$\frac{B(b\to s\gamma)}{B(b\to ce\nu)}=\frac{|V_{ts}^*V_{tb}|^2}{|V_{cb}|^2}\,\frac{6\alpha_{em}}{\pi g(z)}(|C_7(m_b)|^2+|C_7'(m_b)|^2), \tag{67}$$

where $g(z)=1-8z^2+8z^6-z^8-24z^4\ln z$, with $z=m_c/m_b$, is a phase-space factor arising in the semileptonic branching ratio. In order to illustrate the constraints imposed by (66) on the parameters of top-color models, we plot the allowed region in the $D_L^{bs}*/V_{ts}^*-D_R^{bs}*/V_{ts}^*$ plane for fixed values of the charged top-pion and charged scalar masses, $m_{\tilde{\pi}^\pm}$ and $m_{\tilde{H}^\pm}$. The top-pion mass arises through the couplings of the top quark to the Higgs boson, which are proportional to $\epsilon$ and constitute an explicit breaking of chiral symmetry. Estimates of this mass in the fermion loop approximation and consistent with (45) give [6] $m_{\tilde{\pi}^\pm}\approx$ (180–250) GeV. On the other hand, $m_{\tilde{H}^\pm}$ can be estimated using (46). The main contribution to it comes from the top-color interactions. For instance, in [11] it was shown that near criticality and in this approximation it could be as small as $m_{\tilde{H}^\pm}\approx 350$ GeV. We show the constraints from $b\to s\gamma$ for this value as well as for $m_{\tilde{H}^\pm}=1$ TeV in Fig. 2, where $D_L^{bs}*/V_{ts}^*$ is assumed to be real. The data are more constraining for larger values of $m_{\tilde{H}^\pm}$. This is due to a partial cancellation of the top-color effects in (62) and (63), which is more efficient for lighter scalar masses. The second term in (62) reduces the value of $C_7(M_W)$ with respect to the SM for an important range of values of $m_{\tilde{H}^\pm}$. This can be appreciated in Fig. 3, where the rate is plotted versus $m_{\tilde{H}^\pm}$ for different values of $m_{\tilde{\pi}^\pm}$ and for $D_L^{bs}*/V_{ts}^*=1/2$ and $D_R^{bs}=0$. Nonzero values of $D_R^{bs}$ would compensate the cancellation bringing the rate back up in better agreement with experiment, given that $C_7'$ always contributes positively to the rate.

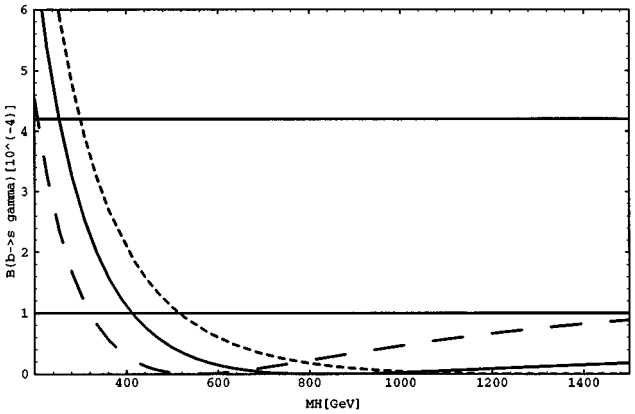


FIG. 3. The predictions for the $b\to s\gamma$ branching ratio in the top-color model I as a function of $m_{\tilde{H}^\pm}$. In this figure we have taken $D_L^{bs}/V_{ts}=0.5$, $D_R^{bs}/V_{ts}=0$, $m_b^*=0.8m_b$, $m_t=175$ GeV. The top-pion mass is taken to be $m_{\tilde{\pi}^\pm}=180$ GeV (dashed), $m_{\tilde{\pi}^\pm}=240$ GeV (solid), and $m_{\tilde{\pi}^\pm}=300$ GeV (dotted). The horizontal lines correspond to the 95% C.L. upper and lower limits from Ref. [15].

Although a large region is still allowed for any given pair of $\tilde{\pi}^+$ and $\tilde{H}^+$ masses, the data are already constraining $D_L^{bs}*/V_{ts}^*$ to be positive or small. A simple ansatz for the mixing matrices $D_L$ and $D_R$ is to assume they are of the order of the square root of the CKM mixing matrix. This gives $|D_{L,R}^{bs}|\simeq(1/2)|V_{ts}|$. As a reference, this is indicated by the square in Fig. 2. Triangular textures as the ones discussed in Sec. II C, allow one of the mixing factors to be very small. The $b\to s\gamma$ data then implies a constraint on the other factor that can be extracted from Fig. 2. These textures seem to be necessary to accommodate $B^0$-$\bar{B}^0$ mixing, as we will see next.

### B. Constraints from nonleptonic processes

At low energies the top-color interactions will induce four-quark operators leading to nonleptonic processes. In order to study the phenomenology of these interactions it is useful to divide them in three categories: $DDDD$, $UUDD$, and $UUUU$. Rotation to the mass eigenbasis will give new four-quark operators now involving the second and first families. Although suppressed by mixing factors, these operators can in principle give contributions to low-energy processes. In top-color I, the down-down operators give rise to potentially large corrections to $B_d$ and $B_s$ mixing. They also induce transitions not present in the SM to lowest order in $G_F$, most notably $b\to ssd$, although with very small branching ratios. In the second category, the up-down operators give vertices that induce corrections to processes allowed at tree level in the SM. These corrections are $\sim 10^{-3}$ relative to the SM amplitudes, and are therefore very hard to observe, given that they appear in channels like $b\to ccs$. The effects of the operators in these two categories

are not sizable in top-color II, since the right-handed down quarks do not couple to the strong SU(3) and there is no strong U(1). Finally, in the up-up operators, the most interesting process is $D^0$-$\overline{D^0}$ mixing given that it is extremely suppressed in the SM.

#### 1. $B^0$-$\overline{B^0}$ mixing

The most important effects of the top-color model in $B^0$-$\overline{B^0}$ mixing are due to the scalar sector generated at low energies. They were studied in detail in [11]. The field $\phi_2$ in (24) contains the two neutral $b\overline{b}$ bound states $\tilde{H}^0, A^0$, which in the approximation (48) can be rather light. When the quarks are rotated to their mass eigenbasis, flavor-changing couplings of $\tilde{H}^0, A^0$ are generated. They induce a contribution to the $B^0$-$\overline{B^0}$ mass difference given by [11]

$$\frac{\Delta m_B}{m_B} = \frac{7}{12}\frac{m_t^2}{f_\pi^2 m_{\tilde{H}^0}^2}\delta_{bd} B_B f_B^2, \tag{68}$$

where[1] $\delta_{bd} \simeq |D_L^{bd} D_R^{bd}|$. Using the experimental measurements of $\Delta m_B$ [21] one obtains the bound

$$\frac{\delta_{bd}}{m_{\tilde{H}^0}^2} < 10^{-12}\ \text{GeV}^{-2}. \tag{69}$$

Thus, if $m_{\tilde{H}^0}$ is of the order of a few hundred GeV, then (69) represents an important constraint on the mixing factors. For instance, if one naively uses the ansatz that takes the square root of the CKM mixing matrix for *both* $D_L$ and $D_R$, the bound (69) is violated by 1–2 orders of magnitudes. However, the triangular textures motivated in Sec. II C provide a natural suppression of the effect by producing approximately diagonal $D_L$ *or* $D_R$ matrices. This gives $\delta_{bd} \approx 0$ and avoids the bound altogether.

#### 2. $D^0$-$\overline{D^0}$ mixing

At the charm quark mass scale the dominant effect in flavor-changing neutral currents is due to the flavor-changing couplings of top-pions. In the case of the top-color I model the operator inducing $D^0$-$\overline{D^0}$ mixing can be written as

$$\mathscr{H}_{\text{eff}} = \frac{1}{2m_{\tilde{\pi}^0}^2}\frac{m_t^2}{2f_\pi^2}\delta_{cu}\overline{u}\gamma_5 c\,\overline{u}\gamma_5 c, \tag{70}$$

where $\delta_{cu} = (U_L^{tu*} U_R^{tc})^2$ is the factor arising from the rotation to the mass eigenstates. Here we have for simplicity assumed $U_L^{tu*} U_R^{tc} = U_R^{tu*} U_L^{tc}$, since we are only interested in the order of magnitude of the effect. In the vacuum insertion approximation,

$$\langle \overline{D^0} | \overline{u}\gamma_5 c\,\overline{u}\gamma_5 c | D^0 \rangle = -2 f_D^2 m_D^2, \tag{71}$$

where $f_D$ is the $D$ meson decay constant. Then the contribution of (70) to the mass difference takes the form

$$\Delta m_D^{\text{TopCI}} = \frac{1}{2} f_D^2 m_D \frac{m_t^2}{f_{\tilde{\pi}}^2 m_{\tilde{\pi}^0}^2} |\delta_{cu}|. \tag{72}$$

In the $\sqrt{\text{CKM}}$ ansatz and for a top-pion mass of $m_{\tilde{\pi}^0} = 200$ GeV we obtain

$$\Delta m_D^{\text{TopCI}} \approx 2 \times 10^{-14}\ \text{GeV}, \tag{73}$$

which is approximately a factor of 5 below the current experimental limit of $1.3 \times 10^{-13}$ GeV [21]. On the other hand, the SM predicts $\Delta m_D^{\text{SM}} < 10^{-15}$ GeV [22]. This puts potentially large top-color effects in the discovery window of future high-statistics charm experiments [23].

The effect is even stronger in the top-color II model. In this case the strong coupling of the right-handed top with the left-handed charm quark induces scalar and pseudoscalar top-pion couplings of the form

$$\mathscr{L} = \frac{m_t}{\sqrt{2} f_{\tilde{\pi}}} \overline{c_L}(\pi_s^0 + i\pi_p^0) t_R + \text{H.c.} \tag{74}$$

The operator contributing to $\Delta m_D$ is now

$$\mathscr{H}_{\text{eff}} = -\frac{m_t^2}{f_{\tilde{\pi}}^2 m_{\tilde{\pi}}^2} U_L^{cc} U_R^{tu*} U_L^{cu*} U_R^{tc} \overline{u_L} c_R \overline{u_R} c_L. \tag{75}$$

Using the $\sqrt{\text{CKM}}$ ansatz, one observes that in this case the $D$ meson mass difference is typically larger by a factor $1/\lambda^4$ compared to the top-color I scenario (with the Wolfenstein parameter $\lambda = 0.22$). Thus we estimate

$$\Delta m_D^{\text{TopCII}} \approx \Delta m_D^{\text{TopCI}} \frac{1}{\lambda^4} \sim 10^{-11}\ \text{GeV}, \tag{76}$$

which violates the current experimental upper limit by about 2 orders of magnitude. This is the single most constraining piece of phenomenology on the top-color II model. However, once again, these constraints can be avoided in models with triangular textures in the up sector.

### C. Semileptonic processes

We study here the FCNC at tree level induced by the exchange of the $Z'$ arising in top-color I models. The corresponding effective Lagrangian is given in (13). After rotation to the mass eigenstates, (13) generates four-fermion interactions leading to FCNC. With the exception of the effect on the $\Upsilon(1S)$ leptonic branching ratio, the cases considered in what follows are of this type.

#### 1. $\Upsilon(1S) \to l^+ l^-$

Although these processes do not involve FCNC, they still receive additional contributions from $Z'$ exchange in top-color I type models. The resulting modification of the $\tau^+\tau^-$ rate violates lepton universality. Experimental results on $\Upsilon(1S) \to l^+ l^-$ might therefore yield important constraints on model parameters, which are independent of quark mixing factors.

The $\Upsilon(1S) \to l^+ l^-$ amplitude can in general be written as

[1]The numerical coefficient on the right-hand side of expression (68) inadvertently appears as 5/12 in [11], rather than the correct 7/12.

$$\mathscr{A}(\Upsilon(1S)\to l^+l^-)=-\frac{4\pi\alpha}{3M_\Upsilon^2}\langle 0|(\overline{bb})_V|\Upsilon(\epsilon)\rangle \times[r_V(\overline{ll})_V+r_A(\overline{ll})_A]. \tag{77}$$

Note that the axial vector piece of the $b$-quark current does not contribute. For the dominant photon exchange contribution $r_V=1$ and $r_A=0$. In the case of the $\tau$-lepton mode these couplings are modified by the effective $Z'$ interaction in (13) into

$$r_V=1-\frac{3\kappa_1}{16\alpha}\frac{M_\Upsilon^2}{M_{Z'}^2},\quad r_A=-\frac{\kappa_1}{16\alpha}\frac{M_\Upsilon^2}{M_{Z'}^2}. \tag{78}$$

The $Z'$ contribution to the electron and muon modes are suppressed by a factor of $\tan^2\theta'$, which we neglect.

Using (77) and

$$\langle 0|(\overline{bb})_V^\mu|\Upsilon(\epsilon)\rangle=iF_\Upsilon M_\Upsilon\epsilon^\mu, \tag{79}$$

one finds for the decay rate

$$\Gamma[\Upsilon(1S)\to l^+l^-]=\frac{4\pi\alpha^2}{27}\frac{F_\Upsilon^2}{M_\Upsilon}\sqrt{1-4\frac{m^2}{M_\Upsilon^2}} \times\left[r_V^2\left(1+2\frac{m^2}{M_\Upsilon^2}\right)+r_A^2\left(1-4\frac{m^2}{M_\Upsilon^2}\right)\right], \tag{80}$$

where $m$ is the lepton mass. From (78) and (80) we see that the leading $Z'$ effect is given by the interference of the $Z'$ exchange with the photon amplitude. This interference is destructive, reducing the $\tau$ rate in comparison with the electron and muon modes according to

$$\frac{\Gamma(\Upsilon(1S)\to\tau^+\tau^-)}{\Gamma(\Upsilon(1S)\to\mu^+\mu^-)}=\sqrt{1-4\frac{m_\tau^2}{M_\Upsilon^2}}\left(1+2\frac{m_\tau^2}{M_\Upsilon^2}\right) \times\left[1-\frac{3}{8}\frac{\kappa_1}{\alpha}\frac{M_\Upsilon^2}{M_{Z'}^2}\right]. \tag{81}$$

In the standard model this ratio is slightly reduced by a phase-space factor which amounts to 0.992. The lepton universality violating $Z'$ effect leads to an additional suppression. For $\kappa_1=1$ and $M_{Z'}=500$ GeV this suppression is $\sim 2\%$. Experimentally, the ratio is measured to be [21,24]

$$\frac{\Gamma(\Upsilon(1S)\to\tau^+\tau^-)}{\Gamma(\Upsilon(1S)\to\mu^+\mu^-)}=1.05\pm 0.07. \tag{82}$$

Presently, the error is still too large for a useful constraint to be derived from this measurement. However, a sensitivity at the percent level, which would start to become binding, does not seem to be completely out of reach. It is interesting to note that the central value in (82) actually exceeds unity. If this feature should persist as the error bar is reduced, it would tend to sharpen the constraint on the negative $Z'$ effect discussed above. Generally speaking, it seems quite plausible that a decay like $\Upsilon(1S)\to\tau^+\tau^-$ could potentially yield important constraints on new strong dynamics associated with the third generation. We have illustrated such a possibility within the framework of the top-color I scenario. In any case, a more precise measurement of the ratio in (82) could give useful information on this type of physics and is very desirable.

### 2. $B_s\to l^+l^-$

The part of the effective interaction given in (13) that is inducing $B_s\to\tau^+\tau^-$ can be written as

$$\mathscr{L}_{\mathrm{eff}Z'}=\frac{\pi\kappa_1}{12M_{Z'}^2}(D_L^{bb*}D_L^{bs}(\overline{bs})_{V-A} -2D_R^{bb*}D_R^{bs}(\overline{bs})_{V+A})[(\overline{\tau\tau})_{V-A}+2(\overline{\tau\tau})_{V+A}] \tag{83}$$

after performing the rotation to mass eigenstates. Using the fact that only the axial vector part of the quark current contributes to the hadronic matrix element and

$$\langle 0|\overline{b}\gamma_\mu\gamma_5 s|B_s(P_\mu)\rangle=if_{B_s}P_\mu, \tag{84}$$

the top-color contribution to the amplitude for $B_s\to\tau^+\tau^-$ is

$$\mathscr{A}^{\mathrm{TopC}}(B_s\to\tau^+\tau^-)=\frac{\pi\kappa_1}{12M_{Z'}^2}\delta_{bs}f_{B_s}P_\mu \times[(\overline{\tau\tau})_{V-A}+2(\overline{\tau\tau})_{V+A}], \tag{85}$$

where we defined

$$\delta_{bs}=D_L^{bb*}D_L^{bs}+2D_R^{bb*}D_R^{bs}. \tag{86}$$

Assuming that only top-color contributes, the width is given by

$$\Gamma(B_s\to\tau^+\tau^-)=\frac{\pi\kappa_1^2}{288M_{Z'}^4}f_{B_s}^2m_{B_s}m_\tau^2|\delta_{bs}|^2\sqrt{1-4\frac{m_\tau^2}{m_{B_s}^2}}. \tag{87}$$

Using $f_{B_s}=0.23$ GeV one gets

$$\Gamma(B_s\to\tau^+\tau^-)=7\times10^{-3}|\delta_{bs}|^2\frac{\kappa_1^2}{M_{Z'}^4}\ \mathrm{GeV}^5. \tag{88}$$

For the neutral mixing factors we make use of the CKM square-root ansatz ($\sqrt{\mathrm{CKM}}$). This choice is rather general in this case given that (86) involves a sum of left and right contributions and will not vanish when the textures are triangular as in (23). We still have the freedom of the relative sign between the elements of $D_L$ and $D_R$ in (86). This introduces an uncertainty of a factor of 3 in the amplitude. Taking $\kappa_1\simeq 1$ we get

$$B(B_s\to\tau^+\tau^-)\approx\begin{cases}1(0.1)\times10^{-3} & \text{for } M_{Z'}=500\ \mathrm{GeV},\\ 6(0.7)\times10^{-5} & \text{for } M_{Z'}=1000\ \mathrm{GeV},\end{cases} \tag{89}$$

where we have used the positive (negative) relative sign in (86). The SM prediction is $B^{\mathrm{SM}}\approx10^{-6}$ [25,26].

On the other hand, first- and second-generation leptons couple to the weaker $U(1)_{Y2}$. The corresponding amplitudes are similar to (85) with $\tau$ replaced by $e$ or $\mu$, except that they carry an additional factor of $(-\tan^2\theta')$. For instance, for $B_s\to\mu^+\mu^-$ one obtains

$$B(B_s\to\mu^+\mu^-)=\left(\frac{m_\mu}{m_\tau}\right)^2\left(1-4\frac{m_\tau^2}{m_{B_s}^2}\right)^{-1/2}\tan^4\theta' \times B(B_s\to\tau^+\tau^-). \quad (90)$$

The choice $\kappa_1=1$ corresponds to $\tan\theta'\approx 0.1$. This gives a suppression factor of $\approx 5\times 10^{-7}$ with respect to the $\tau$ mode. Of this suppression, a factor of $3.5\times 10^{-3}$ comes from helicity. This is not present in the $b\to s l^+ l^-$ decays, which makes the $\mu$ modes more accessible. The SM predicts $B^{\rm SM}(B_s\to\mu^+\mu^-)\approx 4\times 10^{-9}$ [25,26].

Finally, the rates for the $B_d$ purely leptonic modes are obtained by replacing $D^{bs}_{L,R}$ by $D^{bd}_{L,R}$. In the $\sqrt{\rm CKM}$ ansatz this represents a suppression of $\approx 10^{-2}$ in the branching fractions with respect to the $B_s$ case.

### 3. $B\to X_s l^+ l^-$

Using the normalization of the effective Hamiltonian as in (59), the operators contributing to these processes are $O_7$, as given by Eq. (60), and

$$O_9=\frac{e^2}{16\pi^2}(\bar{s}\gamma_\mu b_L)(\bar{l}\gamma^\mu l),$$

$$O_{10}=\frac{e^2}{16\pi^2}(\bar{s}\gamma_\mu b_L)(\bar{l}\gamma^\mu\gamma_5 l). \quad (91)$$

The contact interaction induced by the $Z'$ exchange gives new contributions to the coefficient functions $C_9$ and $C_{10}$ at $\mu=M_W$ as well as nonzero values for the coefficients of the new operators [27]

$$O'_9=\frac{e^2}{16\pi^2}(\bar{s}\gamma_\mu b_R)(\bar{l}\gamma^\mu l), \quad (92)$$

$$O'_{10}=\frac{e^2}{16\pi^2}(\bar{s}\gamma_\mu b_R)(\bar{l}\gamma^\mu\gamma_5 l). \quad (93)$$

These are given by

$$C_9^{\rm TopC}(M_W)=\frac{1}{2}\frac{D_L^{bs*}D_L^{bb}}{V_{ts}^*V_{tb}}F, \quad (94)$$

$$C_{10}^{\rm TopC}(M_W)=\frac{1}{6}\frac{D_L^{bs*}D_L^{bb}}{V_{ts}^*V_{tb}}F, \quad (95)$$

$$C_9'^{\rm TopC}(M_W)=-1\frac{D_R^{bs*}D_R^{bb}}{V_{ts}^*V_{tb}}F, \quad (96)$$

$$C_{10}'^{\rm TopC}(M_W)=-\frac{1}{3}\frac{D_R^{bs*}D_R^{bb}}{V_{ts}^*V_{tb}}F, \quad (97)$$

where we defined

$$F=\frac{4\pi^2 v_w^2}{\alpha}\frac{\kappa_1}{M_{Z'}^2}. \quad (98)$$

Here $v_w^2=(2\sqrt{2}G_F)^{-1}=(174\ {\rm GeV})^2$. (Note that in this section it is assumed that an adequate order-of-magnitude estimate of the novel effects can be obtained by only considering the consequences of $Z'$ exchange. In particular, the scalar bound-state contributions to the coefficient functions $C_7$ and $C_7'$ [cf. Eqs. (62) and (63)] are not taken into account.) Equation (98) applies to the case of the $\tau$ lepton. For $e$ or $\mu$, $F$ carries an additional factor of $(-\tan^2\theta')\approx -0.01$. The dilepton mass distribution has the form

$$\frac{dB(b\to s l^+ l^-)}{ds}=K(1-s)^2\sqrt{1-\frac{4x}{s}}\Bigg\{(|C_9|^2+|C_9'|^2-|C_{10}|^2-|C_{10}'|^2)6x+(|C_9|^2+|C_9'|^2+|C_{10}|^2+|C_{10}'|^2)\times\left[(s-4x)+\left(1+\frac{2x}{s}\right)(1+s)\right]+12C_7{\rm Re}[C_9]\left(1+\frac{2x}{s}\right)+\frac{4|C_7|^2}{s}\left(1+\frac{2x}{s}\right)(2+s)\Bigg\}, \quad (99)$$

where $s=q^2/m_b^2$ and $x=m_l^2/m_b^2$. The factor $K$ is given by

$$K=\frac{\alpha^2}{4\pi^2}\left|\frac{V_{ts}^*V_{tb}}{V_{cb}}\right|^2\frac{B(b\to ce\nu)}{g(z)}, \quad (100)$$

where the function $g(z)$, $z=m_c/m_b$, can be found after Eq. (67). The SM contributions to $b\to s l^+ l^-$ reside in the coefficients $C_7, C_9$, and $C_{10}$. For the present discussion we will neglect QCD effects. This gives a reasonable approximation, which is completely sufficient for our purposes. We use here the coefficient functions from [28] in the limit of vanishing $\alpha_s$. To illustrate the possible size of the new physics effect we choose again the $\sqrt{\rm CKM}$ ansatz. In this case we also have to choose the sign of $D_L^{bs}$, which is taken to be positive. Furthermore we set $\kappa_1=1$. To estimate the order of magnitude of the branching ratios, we simply integrate the dilepton invariant mass spectrum in (99) from $4x$ to 1. Numerical results are given in Table I. The branching ratios are similar to those for $B_s\to\tau^+\tau^-$, given that the partial helicity suppression is balanced by the phase-space suppression in the three-body decay. There are no presently published limits on any of the $\tau$ channels. On the other hand, the angular information in these decays provides a sensitive test of the chiral-

ity of the operators involved. This is true not only for the inclusive decays [29] but also for exclusive modes like $B\to K^* l^+ l^-$, where the SM lepton asymmetry is very distinct in a region where hadronic matrix elements can be reliably predicted [27,30].

#### 4. $B\to X_s \nu\bar{\nu}$

The decay $b\to s\nu\bar{\nu}$ could have an important contribution from the $\tau$ neutrino which couples strongly to the $\mathrm{U}(1)_1$ in top-color I models. The top-color amplitude can be derived from (13) and reads

$$\mathscr{A}^{\mathrm{TopC}}(b\to s\nu_\tau\bar{\nu}_\tau)=-\frac{\pi\kappa_1}{12M_{Z'}^2}[g_v(\bar{s}b)_V+g_a(\bar{s}b)_A]\times(\bar{\nu}_\tau\nu_\tau)_{V-A}, \tag{101}$$

where

$$g_v=D_L^{bb}D_L^{bs*}-2D_R^{bb}D_R^{bs*},$$

$$g_a=-(D_L^{bb}D_L^{bs*}+2D_R^{bb}D_R^{bs*}).$$

On the other hand, the SM amplitude is

$$\mathscr{A}^{\mathrm{SM}}(b\to s\nu_\tau\bar{\nu}_\tau)=\frac{G_F}{\sqrt{2}}\frac{\alpha}{2\pi\sin^2\theta_W}V_{ts}^*V_{tb}X(x_t)\times(\bar{s}b)_{V-A}(\bar{\nu}_\tau\nu_\tau)_{V-A}, \tag{102}$$

where $x_t=m_t^2/M_W^2$ and the Inami-Lim function $X(x)$ is given by

$$X(x)=\frac{x}{8}\left[-\frac{2+x}{1-x}+\frac{3x-6}{(1-x)^2}\ln x\right]. \tag{103}$$

Taking the mixing factors to be

$$\delta_{bs}=D_L^{bb}D_L^{bs*}=D_R^{bb}D_R^{bs*}\sim\frac{1}{2}|V_{ts}|\sim\frac{1}{2}|V_{cb}|, \tag{104}$$

we have

$$\left|\frac{\mathscr{A}_{\mathrm{TopC}}}{\mathscr{A}_{\mathrm{SM}}}\right|=\frac{2\pi^2\sin^2\theta_W v_w^2}{3\alpha X(x_t)}\frac{\kappa_1}{M_{Z'}^2}\frac{\sqrt{|g_v|^2+|g_a|^2}}{\sqrt{2}|V_{ts}^*V_{tb}|}\approx 4\times10^6\ \mathrm{GeV}^2\frac{\kappa_1}{M_{Z'}^2}. \tag{105}$$

The square of this ratio divided by the number of neutrinos gives an estimate of the ratio of branching ratios. We obtain

$$\frac{B^{\mathrm{TopC}}(b\to s\nu_\tau\bar{\nu}_\tau)}{B^{\mathrm{SM}}(b\to s\nu\bar{\nu})}\sim\begin{cases}93\kappa_1^2 & \text{for } M_{Z'}=500\ \mathrm{GeV},\\ 6\kappa_1^2 & \text{for } M_{Z'}=1000\ \mathrm{GeV}.\end{cases} \tag{106}$$

Estimates of this mode in the SM give $B^{\mathrm{SM}}\simeq 4.5\times10^{-5}$ [25,26].

#### 5. $K^+\to\pi^+\nu\bar{\nu}$

As in $B\to X_s\nu\bar{\nu}$, we are concerned with the contact term involving $\tau$ neutrinos, given that they constitute the most important top-color contribution. The top-color amplitude is given by

$$\mathscr{A}^{\mathrm{TopC}}(K^+\to\pi^+\nu_\tau\bar{\nu}_\tau)=-\frac{\pi\kappa_1}{12M_{Z'}^2}\delta_{ds}\langle\pi^+(k)|(\bar{s}d)_V|K^+(p)\rangle\times(\bar{\nu}_\tau\nu_\tau)_{V-A}, \tag{107}$$

where now $\delta_{ds}=D_L^{bs}*D_L^{bd}-2D_R^{bs}*D_R^{bd}$. The hadronic matrix element in (107) can be written in terms of the one entering the semileptonic decay

$$\langle\pi^+(k)|(\bar{s}d)_V^\mu|K^+(p)\rangle=\sqrt{2}\langle\pi^0(k)|(\bar{s}u)_V^\mu|K^+(p)\rangle=f_+(q^2)(p+k)^\mu \tag{108}$$

and the form factor $f_+(q^2)$ is experimentally well known. In any case it will cancel when taking the ratio to the SM amplitude. For one neutrino species this is given by

$$\mathscr{A}^{\mathrm{SM}}(K^+\to\pi^+\nu_\tau\bar{\nu}_\tau)=\frac{G_F}{\sqrt{2}}\frac{\alpha}{2\pi\sin^2\theta_W}\sum_{j=c,t}V_{js}^*V_{jd}X(x_j)\times\langle\pi^+|(\bar{s}d)_V|K^+\rangle(\bar{\nu}_\tau\nu_\tau)_{V-A}, \tag{109}$$

where $x_j=m_j^2/M_W^2$ and $X(x)$ is the Inami-Lim function defined in (103). Here we have neglected QCD corrections and the $\tau$-lepton mass effects. Since only the vector quark current contributes to the exclusive transition, the Dirac structure in the top-color and SM amplitudes is the same. The ratio of the top-color amplitude to the SM is then

$$\left.\frac{\mathscr{A}_{\mathrm{TopC}}}{\mathscr{A}_{\mathrm{SM}}}\right|_{\nu_\tau}=-\frac{2\pi^2\sin^2\theta_W v_w^2}{3\alpha}\frac{\kappa_1}{M_{Z'}^2}\frac{\delta_{ds}}{S}, \tag{110}$$

where we defined

$$S=\sum_{j=c,t}V_{js}^*V_{jd}\,X(x_j). \tag{111}$$

For $m_t=175$ GeV, we have $|S|\approx10^{-3}$ and the ratio can be expressed as

TABLE I. Estimates of inclusive branching ratios for $b\to s l^+ l^-$ in the SM and the top-color model I.

| $M_{Z'}$ (GeV) | $B(b\to s\tau^+\tau^-)$ | $B(b\to s\mu^+\mu^-)$ |
|---|---|---|
| 500 | $1.4\times10^{-3}$ | $6.7\times10^{-6}$ |
| 1000 | $0.9\times10^{-4}$ | $6.0\times10^{-6}$ |
| SM | $3.7\times10^{-7}$ | $6.3\times10^{-6}$ |

$$\left|\frac{\mathscr{A}^{\mathrm{TopC}}}{\mathscr{A}^{\mathrm{SM}}}\right|_{\nu_\tau} = 6\times 10^9 |\delta_{ds}| \frac{\kappa_1}{M_{Z'}^2}\ \mathrm{GeV}^2. \tag{112}$$

The $\sqrt{\mathrm{CKM}}$ ansatz yields

$$\delta_{ds} = -\frac{1}{4}\lambda^5\left(\frac{3}{4}\lambda^5\right) \tag{113}$$

when choosing positive (negative) relative signs between the two terms entering in $\delta_{ds}$. This gives, for $M_{Z'}=500$ GeV and $\kappa_1=1$, a ratio of amplitudes which is about 3 (9).

In the SM one expects $B(K^+\to\pi^+\nu\overline{\nu})\sim 10^{-10}$ [31]. Presently, the experimental upper limit is $5.2\times 10^{-9}$ [21]. Experiments are under way at Brookhaven National Laboratory (BNL) to reach the sensitivity necessary to observe $K^+\to\pi^+\nu\overline{\nu}$ if it occurs at the SM level [32]. Any significant deviation from the SM expectation should then also show up in these experiments.

## V. CONCLUSIONS

In this paper we have given a treatment of the low-energy phenomenological implications of top-color models, with possible generic implications of extended technicolor schemes. We have also given an effective Lagrangian analysis of the bound states in top-color models. This provides a point of departure for further studies. For example, we have not examined the question of whether the $\theta$ term in TopC gives rise to novel, non-CKM observable $CP$ violation. The potentially observable effects we have considered arise because the current basis of quarks and leptons of the third generation experiences new strong forces. When we diagonalize the mass matrix to arrive at the mass basis there will be induced flavor-changing interactions. These are largely amplified by the bound-state formation, e.g., effects such as $BB$ mixing are induced by coloron exchange, but the formation of low-mass top pions gives the dominant contribution in a channel contained by the coloron exchange. Hence, it really suffices to consider the dominant effect in the context of the effective Lagrangian. In the semileptonic processes the effects are controlled by the $Z'$ exchange, and the top-pion effects are not dominant. Top-color, to an extent, explains the suppression of the $3\to 2,1$ mixing angles, though without further assumptions about the origin of generational structure it cannot distinguish between first and second generations.

We have also sketched how the top-color scheme can impose textures upon the mass matrix which is inevitable due to the gauge quantum numbers that distinguish generations. A chiral-triangular texture emerges as a natural possibility which can suppress dangerous processes such as $BB$ mixing. Without this natural source of FCNC suppression, the model would require fine-tuning or an *ad hoc* texture assumption.

We view top-color as a family of models. We have discussed two classes: Top-color I models which involve an additional $\mathrm{U}(1)'$ to tilt the chiral condensate into the $tt$ flavor direction; top-color II, based upon the gauge group $\mathrm{SU}(3)_Q\times\mathrm{SU}(3)_1\times\mathrm{SU}(3)_2\times\mathrm{U}(1)_Y\times\mathrm{SU}(2)_L$, where there is only the conventional $\mathrm{U}(1)_Y$, and no strong additional U(1). These latter models admit a rather intriguing anomaly cancellation solution in which the $(c,s)_{L,R}$ doublets are treated differently under the strong $\mathrm{SU}(3)_1\times\mathrm{SU}(3)_2$ structure and a triplet of ''$Q$ quarks'' occurs which can condense to break top-color. Top-color I has a number of sensitive implications in semileptonic processes which we have detailed; top-color II gives only a handful of novel effects in nonleptonic processes, most notably in $D^0$-$\overline{D^0}$ mixing.

In general, it appears that top-color does not produce an overwhelming degree of obvious new physics in the low-energy spectrum. Therefore, significant GIM-violating dynamics in the third generation does not seem to imply large observable deviations from the standard model in low-energy experiments at present. The most sensitive effects are semileptonic and trace to the more model dependent $Z'$. These effects may be shared by other generational U(1) models (e.g., Holdom's [12]). The purely nonleptonic effects are harder to disentangle from electroweak physics. Thus, the electroweak scale itself and the scale of the top-quark mass are places to look for the new physics. Our analysis shows that dramatic new physics can emerge at high-$p_T$ in the third generation having eluded detection in sensitive low-energy experiments. However, in a large number of future high statistics experiments there are potential signatures of this new physics and these should be sought.

## ACKNOWLEDGMENTS

This work was performed at the Fermi National Accelerator Laboratory, which is operated by Universities Research Association, Inc., under Contract No. DE-AC02-76CHO3000 with the U.S. Department of Energy. D.K. thanks the Fermilab Theory Group for their warm hospitality. He further acknowledges support from NSF Contract No. PHY-9057173 and DOE Contract No. DE-FG02-91ER40676 (while at Boston University) and from the German DFG under Contract No. Li519/2-1.

[1] S. Weinberg, Phys. Rev. D **13**, 974 (1976); L. Susskind, *ibid.* **20**, 2619 (1979); S. Dimopoulos and L. Susskind, Nucl. Phys. **B155**, 237 (1979); E. Eichten and K. Lane, Phys. Lett. **90B**, 125 (1980).

[2] B. Holdom, Phys. Rev. Lett. **60**, 1223 (1988); see also [3].

[3] T. Appelquist, M. Einhorn, T. Takeuchi, and L. C. R. Wijewardhana, Phys. Lett. B **220**, 223 (1989); T. W. Appelquist, D. Karabali, and L. C. R. Wijewardhana, Phys. Rev. Lett. **57**, 957 (1986); R. R. Mendel and V. Miransky, Phys. Lett. B **268**, 384 (1991); V. Miransky, Phys. Rev. Lett. **69**, 1022 (1992); N. Evans, Phys. Lett. B **331**, 378 (1994).

[4] E. Eichten and K. Lane, Phys. Lett. B **222**, 274 (1989); K. Lane and M. Ramana, Phys. Rev. D **44**, 2678 (1991).

[5] C. T. Hill, Phys. Lett. B **266**, 419 (1991).

[6] C. T. Hill, Phys. Lett. B **345**, 483 (1995).

[7] S. P. Martin, Phys. Rev. D **46**, 2197 (1992); **45**, 4283 (1992);

Nucl. Phys. **B398**, 359 (1993); M. Lindner and D. Ross, Nucl. Phys. **B370**, 30 (1992); R. Bönisch, Phys. Lett. B **268**, 394 (1991); C. T. Hill, D. Kennedy, T. Onogi, and H. L. Yu, Phys. Rev. D **47**, 2940 (1993).

[8] W. A. Bardeen, C. T. Hill, and M. Lindner, Phys. Rev. D **41**, 1647 (1990).

[9] R. S. Chivukula, B. A. Dobrescu, and J. Terning, Phys. Lett. B **353**, 289 (1995).

[10] K. Lane and E. Eichten, Phys. Lett. B **352**, 382 (1995).

[11] D. Kominis, Phys. Lett. B **358**, 312 (1995).

[12] B. Holdom, ''New Third Family Flavor Physics and the Top Mass,'' Report No. UTPT-95-13, HEP-PH 9506428, 1995 (unpublished); B. Holdom and M. V. Ramana, Phys. Lett. B **365**, 309 (1996).

[13] T. Appelquist and N. Evans, Phys. Rev. D **53**, 2789 (1996).

[14] Y. Nambu and G. Jona-Lasinio, Phys. Rev. **122**, 345 (1961).

[15] CLEO Collaboration, M. Alam *et al.*, Phys. Rev. Lett. **74**, 2885 (1995).

[16] See, e.g., N. Deshpande, in *B-Decays*, edited by S. Stone (World Scientific, Singapore, 1992); J. L. Hewett, in *Spin Structure in High Energy Processes*, Proceedings of the 21st SLAC Summer Institute on Particle Physics, Stanford, California, 1993, edited by L. De Porcel and C. Dunwoodie (SLAC Report No. 444, Stanford, 1994), p. 463; Phys. Rev. Lett. **70**, 1045 (1993); V. Barger, M. Berger, and R. J. N. Phillips, *ibid.* **70**, 1368 (1993).

[17] E. Golowich and S. Pakvasa, Phys. Rev. D **51**, 1215 (1995); J. M. Soares, *ibid.* **53**, 271 (1996).

[18] B. Grinstein, R. Springer, and M. Wise, Nucl. Phys. **B339**, 269 (1990).

[19] M. Ciuchini, E. Franco, G. Martinelli, L. Reina, and L. Silvestrini, Phys. Lett. B **316**, 127 (1993); M. Ciuchini, E. Franco, L. Reina, and L. Silvestrini, Nucl. Phys. **B421**, 41 (1994).

[20] A. J. Buras, M. Misiak, M. Münz, and S. Pokorski, Nucl. Phys. **B424**, 374 (1994).

[21] Particle Data Group, L. Montanet *et al.*, Phys. Rev. D **50**, 1173 (1994).

[22] J. F. Donoghue, E. Golowich, B. Holstein, and J. Trampetic, Phys. Rev. D **33**, 179 (1986); H. Georgi, Phys. Lett. B **297**, 353 (1992); T. Ohl, G. Ricciardi, and E. Simmons, Nucl. Phys. **B403**, 605 (1993); G. Burdman, ''Potential for Discoveries in Charm Meson Physics,'' Fermilab Report No. FERMILAB-CONF-95-281-T, HEP-PH 9508349 (unpublished).

[23] D. M. Kaplan, ''High Impact Charm Physics at the Turn of the Millenium,'' Report No. IIT-HEP-95-3, HEP-EX 9508018 (unpublished).

[24] CLEO Collaboration, D. Cinabro *et al.*, Phys. Lett. B **340**, 129 (1994).

[25] G. Buchalla and A. J. Buras, Nucl. Phys. **B400**, 225 (1993); G. Buchalla, A. J. Buras, and M. E. Lautenbacher, ''Weak Decays Beyond Leading Logarithms,'' Fermilab Report No. FERMILAB-PUB-95/305-T (unpublished).

[26] A. Ali, C. Greub, and T. Mannel, in *B-Physics Working Group Report*, Proceedings of the ECFA Workshop on a European B-Meson Factory, Hamburg, Germany, 1993, edited by R. Aleksan and A. Ali (ECFA Report No. 93-151, Hamburg, 1993).

[27] G. Burdman, Phys. Rev. D **52**, 6400 (1995).

[28] A. J. Buras and M. Münz, Phys. Rev. D **52**, 186 (1995).

[29] A. Ali, T. Mannel, and T. Morozumi, Phys. Lett. B **273**, 505 (1991).

[30] D. Liu, Phys. Lett. B **346**, 355 (1995).

[31] A. J. Buras, M. E. Lautenbacher, and G. Ostermaier, Phys. Rev. D **50**, 3433 (1994).

[32] L. Littenberg and G. Valencia, Annu. Rev. Nucl. Part. Sci. **43**, 729 (1993).